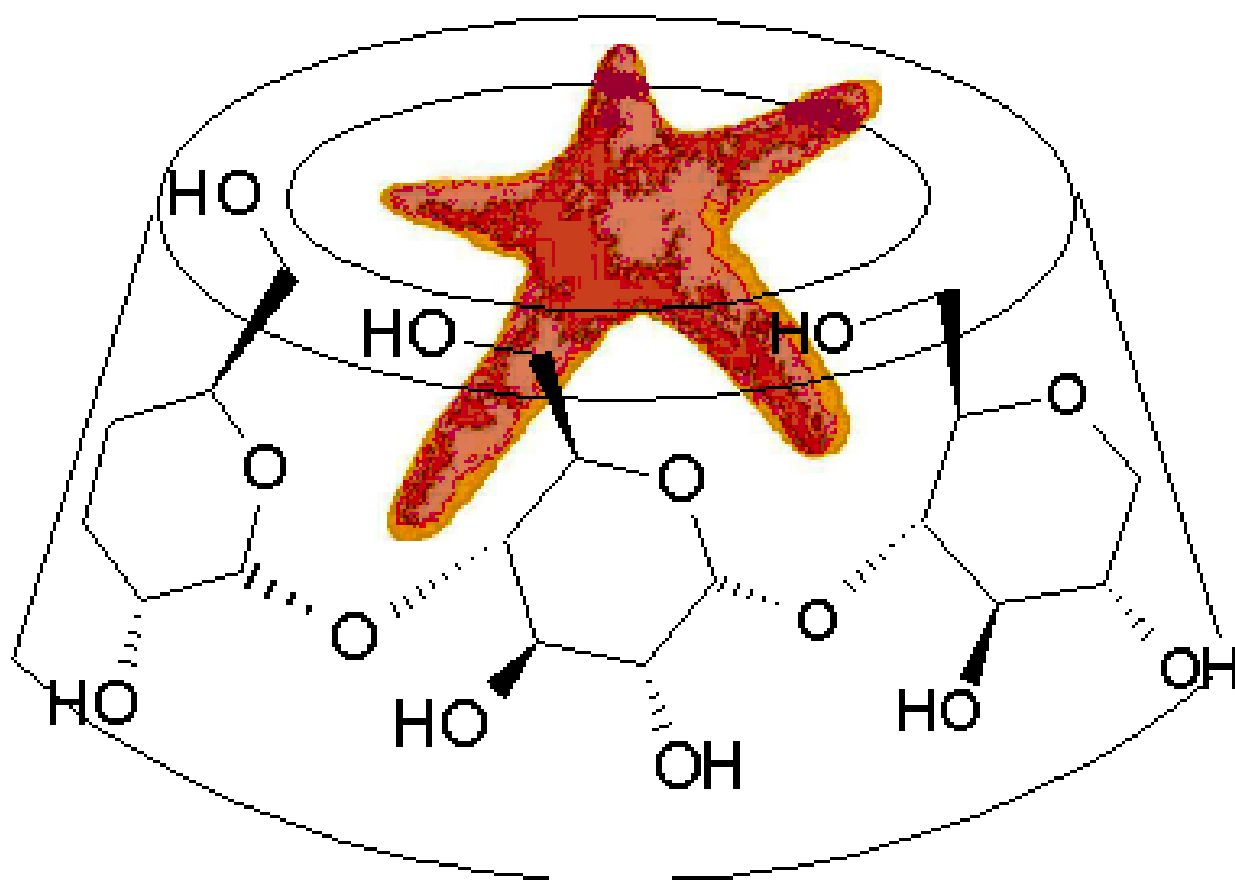


**THE INFLUENCE OF COMPLEX  
FORMATION ON THE DEGRADATION  
OF  $\gamma$ -CYCLODEXTRIN BY  $\alpha$ -AMYLASE**



**LUDMILLA LUMHOLDT RIISAGER**

**MASTER'S THESIS 2010**

**DEPARTMENT OF BIOTECHNOLOGY, CHEMISTRY AND  
ENVIRONMENTAL ENGINEERING**

**AALBORG UNIVERSITY**



**Title**

The influence of complex formation on the degradation of  $\gamma$ -cyclodextrin by  $\alpha$ -amylase

**Master Student**

Ludmilla Lumholdt Riisager

**Supervisor**

Kim Lambertsen Larsen, AAU  
René Holm, H. Lundbeck A/S

**Semester**

K9B-K10B

---

Ludmilla Lumholdt Riisager

Number of copies	6
Number of pages	57
Number of appendices	2

**Abstract**

The purpose of this master's thesis was to investigate the possible influences of complex formation on  $\gamma$ -cyclodextrin ( $\gamma$ -CD) degradation by  $\alpha$ -amylase. It was confirmed that  $\gamma$ -CD is degraded, as the only native CD, by human and porcine pancreatic  $\alpha$ -amylase as well as human salivary  $\alpha$ -amylase, as previously reported. The porcine  $\alpha$ -amylase was found to be the most efficient of the three, consisting with the literature, the human salivary  $\alpha$ -amylase, though, was found to be 1.5 faster than human pancreatic  $\alpha$ -amylase, which is opposite literature reports. Hydroxypropyl- $\gamma$ -CD was found to be degraded by porcine pancreatic  $\alpha$ -amylase, which seemingly has not been shown before.  $\alpha$ -CD was shown to have an inhibiting effect on  $\gamma$ -CD degradation although no consistency between inhibiting effect and  $\alpha$ -CD concentration could be shown at the concentrations examined. Stability constants of complexes between  $\gamma$ -CD and ibuprofen, flurbiprofen, danazol, cinnarizine, halofantrine, and benzo[*a*]pyrene was determined using Higuchi-Connors diagrams and the degradation of  $\gamma$ -CD in the presence of flurbiprofen ( $K_{1:1}$ : 78.4) and benzo[*a*]pyrene ( $K_{1:1}$ : 61,240) was investigated. The conclusion is that the degradation is partly inhibited by the presence of the complex with the stronger complex being degraded more slowly than the weaker complex. Hence, the conclusion is that complex formation does have an influence on the degradation of  $\gamma$ -CD by slowing the degradation. However, the fact that  $\gamma$ -CD is degraded in spite of the complex indicates that, using  $\gamma$ -CD as vehicle, the drug absorption will not be impeded; a situation described by Westerberg & Wiklund (2005). This indicates that  $\gamma$ -CD, is, in fact, a more suitable vehicle for early animal experiments.



# AALBORG UNIVERSITET

Institut for Kemi, Miljø og Bioteknologi  
Sektion for Bioteknologi

## Titel

Kompleksdannelse indflydelse  
på  $\alpha$ -amylases nedbrydelse  
af  $\gamma$ -cyklodextrin

## Kandidatstuderende

Ludmilla Lumholdt Riisager

## Vejleder

Kim Lambertsen Larsen, AAU  
René Holm, H. Lundbeck A/S

## Semester

K9B-K10B

---

Ludmilla Lumholdt Riisager

Oplag	6
Sidetal	57
Bilagsantal	2

## Synopsis

Formålet med dette speciale var at undersøge de mulige effekter af kompleksdannelse på nedbrydelsen af  $\gamma$ -cyklodextriner ( $\gamma$ -CD) med  $\alpha$ -amylase. Det kan konkluderes, at  $\gamma$ -CD, som den eneste native CD, nedbrydes af både svine og human pancreas  $\alpha$ -amylase, såvel som human spyt  $\alpha$ -amylase. Svine  $\alpha$ -amylase viste sig at være den mest effektive af de tre, hvilket er i overensstemmelse med litteraturen. Human spyt  $\alpha$ -amylase viste sig til gengæld at være 1,5 gange hurtigere end human pancreas  $\alpha$ -amylase, hvilket er det modsatte af tidligere publicerede resultater. Det blev vist, at hydroxypropyl- $\gamma$ -CD nedbrydes af svine pancreas  $\alpha$ -amylase, hvilket tilsyneladende ikke er blevet rapporteret før.  $\alpha$ -CD viste sig at have en inhiberende effekt på nedbrydelsen af  $\gamma$ -CD; dog kunne der ved de anvendte koncentrationer ikke påvises en sammenhæng mellem koncentrationen af  $\alpha$ -CD og den inhiberende virkning.

Stabilitetskonstanter af komplekser mellem  $\gamma$ -CD og ibuprofen, flurbiprofen, danazol, cinnarizin, halofantrin, og benzo[*a*]pyren blev bestemt ved hjælp af Higuchi-Connors diagrammer og nedbrydningen af  $\gamma$ -CD ved tilstedeværelse af flurbiprofen ( $K_{1:1}$ : 78,4) og benzo[*a*]pyren ( $K_{1:1}$ : 61.240) blev undersøgt. Det kan konkluderes, at nedbrydningen viste sig at være delvist hæmmet af tilstedeværelsen af komplekset med det stærkere kompleks nedbrudt langsommere end det svagere kompleks. Derfor er konklusionen, at kompleksdannelse har indflydelse på nedbrydningen af  $\gamma$ -CD ved at nedsætte hastigheden. Det faktum, at  $\gamma$ -CD nedbrydes på trods af tilstedeværelsen af komplekset indikerer, at ved brug af  $\gamma$ -CD som vehikel vil medikamentabsorptionen ikke hæmmes; en situation som beskrevet af Westerberg & Wiklund (2005). Dette indikerer, at  $\gamma$ -CD kunne være et mere passende vehikel til brug ved tidlige medicinske dyreforsøg.

# Index

Preface.....	6
1 Introduction.....	7
1.1 Problem statement.....	16
2 Experimental aspects.....	17
2.1 Characterization of inclusion complexes.....	18
3 Materials and methods.....	23
3.1 Determination of complex stability constants.....	23
3.2 Examination of crystal structure of compounds.....	24
3.3 Investigation of degradation of cyclodextrins.....	24
3.4 Investigation of degradation rates of inclusion complexes.....	24
3.5 Influence of $\alpha$ -cyclodextrin on the degradation of $\gamma$ -cyclodextrin.....	24
4 Results and discussion.....	25
4.1 Characterization of complexes.....	25
4.1.1 The complex between benzo[ <i>a</i> ]pyrene and $\gamma$ -cyclodextrin.....	27
4.1.2 The complex between cinnarizine and $\gamma$ -cyclodextrin.....	29
4.1.3 The complex between danazol and $\gamma$ -cyclodextrin.....	30
4.1.4 The complex between flurbiprofen and $\gamma$ -cyclodextrin.....	32
4.1.5 The complex between ibuprofen and $\gamma$ -cyclodextrin.....	34
4.1.6 The complex between halofantrine and $\gamma$ -cyclodextrin.....	37
4.2 The degradation of cyclodextrins by various $\alpha$ -amylases.....	40
4.2.1 Porcine pancreatic $\alpha$ -amylase.....	41
4.2.2 Human pancreatic and salivary $\alpha$ -amylase.....	44
4.2.3 Comparison between the porcine and human amylases.....	45
4.2.4 Degradation of $\gamma$ -cyclodextrin in the presence of $\alpha$ -cyclodextrin.....	46
4.3 The degradation of cyclodextrin inclusion complexes by porcine $\alpha$ -amylase.....	47
5 Conclusion.....	50
6 References.....	51
APPENDIX I.....	55
APPENDIX II.....	57

## **Preface**

This master's thesis was completed at Aalborg University, Department of Biotechnology, Chemistry, and Environmental Engineering and at H. Lundbeck A/S, Preformulation Department.

Citations and references are stated as, (surname of first author, year of publication) according to the Harvard System.

A data disc is enclosed containing raw and processed data, as well as a pdf-version of the thesis.

I would like to thank Klaus Hestehauge for assistance with XRD analysis, and the rest of the Preformulation Department, H. Lundbeck A/S for letting me get in their way, eat their fruit and cakes and, in spite of this, still offering general help and guidance. A special thanks to Erling Jørgensen, same place, a most patient man without whom a lot would have been very, very, very different...

Also thanks to Maria Sigsgaard for proof-reading.

And finally, thanks to Lasse for everlasting patience, lenience, patience, technical assistance, patience, proof-reading, and did I mention patience?

# 1 Introduction

In 1891 a French scientist by the name Villiers isolated a crystalline product from a bacterial digestion of starch. The product was named cellulosine due to its resemblance of cellulose in the resistance against acidic hydrolysis. A decade later Schardinger managed to isolate two different crystalline products, which later would be known as  $\alpha$ -cyclodextrin ( $\alpha$ -CD) and  $\beta$ -cyclodextrin ( $\beta$ -CD), from a starch digestion by an isolated strain of the bacterium he later named *B. macerens*. In the late 1940's and the 1950's more intense studies on physical, chemical and inclusion properties were made and it was also during this period that  $\gamma$ -cyclodextrin ( $\gamma$ -CD) was discovered. But it was also during this time that it became the general perception that cyclodextrins were toxic, based upon an experiment that caused the death of the experimental rats, though the study was probably conducted using contaminated cyclodextrins. Not until the 1970's did more thorough experiments elucidate the fact that cyclodextrins are only toxic in very large amounts and/or in a more indirect manner when complexed with toxic substances. This became the beginning of the extensive industrial use of cyclodextrins today (Szejtli, 1998).

Cyclodextrins (CDs) are cyclic oligosaccharides consisting of glucose units linked together with  $\alpha$ -1,4-glycosidic bonds. The three major CDs are comprised of 6, 7, and 8 glucose units and are called  $\alpha$ -CD,  $\beta$ -CD, and  $\gamma$ -CD, respectively. The glucose units are in the  ${}^4C_1$  conformation so that all the secondary hydroxyl groups are located at one of the edges of the ring and the primary hydroxyl groups at the other. The cavity of the ring is lined with the hydrogen atoms of the C3s and C5s and the ether-like oxygens of the glycosidic bond. Due to the free rotation of the primary hydroxyl groups the effective diameter of the rim at the primary hydroxyl groups is smaller than the rim at the secondary hydroxyl groups giving the CD rings a shape of a truncated cone with a cavity, see figure 1, which also contains geometrical information on the three CDs. The cavity of the CDs is relatively hydrophobic in comparison with water, due to the lining of the hydrogens and the ether-like oxygens. The CDs themselves are water soluble due to the hydroxyl groups at the rims, although to various extents: The water solubility of  $\beta$ -CD is only 1.85 g/100 ml whereas it is 14.5 g/100 ml and 23.2 g/100 ml for  $\alpha$ -CD and  $\gamma$ -CD, respectively, at 25°C. These differences are caused by the formation of internal hydrogen bonds, where the strength depends on the ring size of the CD. OH2 (see figure 1B for reference) of each pyranose ring will form a hydrogen bond with the OH3 in the adjacent ring. In  $\beta$ -CD this will create a completed "sphere" of hydrogen bonds,

which confer a rather rigid structure to the molecule and lower the number of available hydrogen bonds for the solvent leading to the very low water solubility compared to the other two CDs. In  $\alpha$ -CD a distortion of one of the pyranose rings inhibits the creation of a completed sphere and only four of six possible hydrogen bonds are created.  $\gamma$ -CD has, due to its size, a more flexible structure and is therefore the most water soluble of the three (Szejtli, 1998).

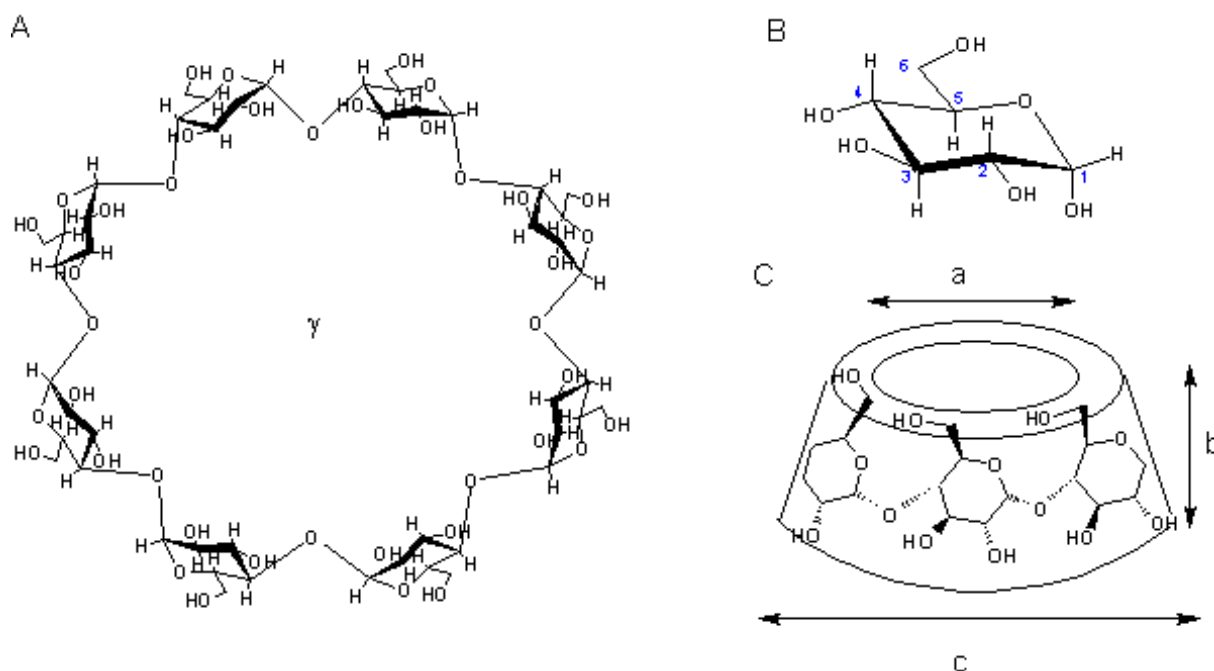


**Figure 1:** A) Structure of  $\gamma$ -cyclodextrin. The structure of  $\alpha$ - and  $\beta$ -cyclodextrin is similar only with six and seven glucose units, respectively. B)  $\alpha$ -D-glucose, the structural unit of cyclodextrins, with numbering of each carbon and thereby the appurtenant hydrogen and hydroxyl group. C) Schematic view of the cyclodextrin torus. Distance a) is the diameter of the cavity and is 4.7-5.3 Å, 6.0-6.5 Å, and 7.5-8.3 Å for  $\alpha$ ,  $\beta$ , and  $\gamma$ , respectively. The height of all tori, distance b, is 7.8 Å, while the outer girth, c, is 14.6 Å, 15.4 Å, and 17.5 Å for  $\alpha$ -,  $\beta$ -, and  $\gamma$ -cyclodextrin, respectively (Szejtli, 1998).

The striking feature of CDs is their cavity. As mentioned earlier the cavity is hydrophobic compared to water and CDs cavity can therefore form inclusion complexes with molecules with a lower polarity than water, thereby improving the solubility of the guest. In solution, the CD cavity is filled to a certain degree with solvent molecules. Even though the solvation of the cavity is far from being ideal, as the water molecules cannot sustain their usual hydrogen bonding conformation when inside the cavity, keeping the cavity of  $\alpha$ -CD empty would require an energy supply of approx. 270 kJ/mole CD. This high number is even higher for  $\beta$ -CD and  $\gamma$ -CD as the volume of their cavity is larger (Szejtli, 1988). The thermodynamic driving forces of complexation are a disputed topic, but it is generally thought to be the result of various parameters, where not all necessarily apply to every CD. For instance, the previous mentioned distortion of  $\alpha$ -CD can act as a driving force since the strain of the ring is loosened



upon complex formation and a more complete hydrogen bond sphere can be created (Harata, 2006). It has been suggested that a driving force of the complexation may be the imperfect solvation of the cavities. The polar/apolar interaction between the cavity and the water is energetically unfavourable so when a more apolar molecule is introduced to the solution, the possible apolar/apolar interaction between this guest and the cavity is more preferred and complex formation happens when the water is replaced by the guest (Szejtli, 1988). On the other hand, it has been argued that although the water bound inside the cavity is at a higher energy level than that on the outside, the negative enthalpy change, obtained by exclusion of the water on complexation, is coupled to a loss of entropy given that the water has a higher conformational freedom inside than outside the cavity. This enthalpy-entropy compensation does not result in a negative Gibbs energy change and is therefore not a driving force for complexation (Liu & Guo, 2002). Liu & Guo (2002) also showed that CDs have reasonably large dipole moments indicating that the Debye force is of great importance to the complexation. It was argued that correlation between complex strength and molecular traits, like size and electron density, indicates that Debye and London forces are involved in the complexation since these forces depends on polarizability which in turn is related to the mentioned traits. This was further established by arguing that the polarizability of water is lower than that the cavity, meaning that the mentioned van der Waal forces must be stronger between CD and guest than between water and guest. The fact that it is repeatedly observed that CDs include the most apolar parts of a molecule and that increasing hydrophobicity leads to increasing complexation led to the conclusion that hydrophobic interaction is another major driving force. In general, all van der Waal forces as well as hydrophobic interactions were declared as driving forces of inclusion complexation with London, Debye, and hydrophobic interactions being the main contributors. Depending on the guest and relevant CD substitutions, hydrogen bonding may also be of importance (Liu & Guo, 2002).

Although CDs are made from starch and share structural features, the degradation pattern is quite different. While starch is degraded completely by several glycosyl hydrolases, the only glycosyl hydrolase capable of degrading CDs is  $\alpha$ -amylase, a family 13 member according to the classification of Henrissat (1991), and only to various extents.  $\alpha$ -amylase has endo activity and hydrolyzes  $\alpha$ -1,4-glycosidic bonds of, as mentioned, mainly starch producing  $\alpha$ -limit dextrans and oligosaccharides (van der Maarel *et al.*, 2002). However, very little work has been done on the subject of the degradation of CDs by  $\alpha$ -amylase. Abdullah *et al.* (1966)

investigated the mode of action of porcine  $\alpha$ -amylase and used  $\gamma$ -CD as a substrate. Abdullah and co-workers concluded that the enzyme uses a multiple attack mechanism when hydrolyzing the substrates, but no detailed investigation on the reaction itself were made and hence, no conclusions were made regarding the rate of hydrolysis. Jodál *et al.* (1984a and 1984b) made a comparison between the kinetic parameters of the degradation reactions of  $\alpha$ -,  $\beta$ -, and  $\gamma$ -CD (using an  $\alpha$ -amylase from *Aspergillus oryzae*) as well as an investigation of the composition and distribution of hydrolysis products. The reported results showed that  $\gamma$ -CD was completely hydrolysed after 24 hours into mainly maltotriose, maltose, and glucose.  $\alpha$ -CD and  $\beta$ -CD were only partial degraded with 98% and 83% unreacted CD remaining, respectively after the 24 hours. The degraded fractions had been converted to glucose and maltose and, in the case of  $\beta$ -CD, maltotriose. However, it was discovered that the degradation reaction also resulted in higher oligosaccharides, like maltotetraose and higher, but hypothesised that these higher oligosaccharides might function as inhibitors of the reaction (Jodál *et al.*, 1984a). This hypothesis was confirmed by studying the kinetic parameters in the presence of each of the oligosaccharides. While maltopentaose and hexaose functioned as substrates the smaller oligosaccharides (glucose, maltose, maltotriose, and maltotetraose) all showed inhibitory effects. By adding various concentrations of the larger oligosaccharides as inhibitor and following the degradation analysis by Lineweaver-Burk plots showed increased  $K_M$ -values thus indicating a competitive inhibition, possibly due to occupation of the active site of the amylase as a result of their relative resemblance to native CDs. The smaller oligosaccharides exhibited a non-competitive inhibition, expressed by a constant  $K_M$ , but decreasing  $V_{max}$ , which reflects that these compounds are too small to be substrates of the enzyme. Instead, they bind to an allosteric site on the enzyme thereby hampering the reaction causing  $V_{max}$  to decrease (Jodál *et al.*, 1984b). However, as mentioned above, Jodál *et al.* (1984a+b) used an  $\alpha$ -amylase from the fungus *A. oryzae* in both studies which means, the results are not necessarily comparable to mammal  $\alpha$ -amylase. For instance, *A. oryzae*  $\alpha$ -amylase does not exhibit the multiple attack mode of action as the porcine amylase does (Abdullah *et al.*, 1966). The degradation of CDs by some mammal  $\alpha$ -amylases has been investigated by Marshall & Miwa (1991) and Kondo *et al.* (1981). The former showed a degradation of  $\gamma$ -CD by human pancreatic and salivary  $\alpha$ -amylase (HPA and HSA, respectively) and a very limited degradation of  $\alpha$ - and  $\beta$ -CD. Focus was then directed towards the kinetic difference between the degradation of  $\gamma$ -CD by the two amylases and reported that

HPA has a lower  $K_M$  and higher  $V_{max}$  values than HSA indicating a higher specific activity of HPA than that of HSA. Measurements of the reaction products after 30 minutes further confirmed this by showing that the hydrolysis reaction was more advanced with HPA than HSA. They also confirmed that the mode of action is multiple attacks and showed that the pH optimum for the reaction is 5.0 (Marshall & Miwa, 1981). Kondo *et al.* (1981) used a protocol similar to the one used by Jodal *et al.* (1984 a+b) though they used HPA, HSA, and a porcine pancreatic  $\alpha$ -amylase (PPA). Kondo *et al.* (1981) also demonstrated that only  $\gamma$ -CD and not  $\alpha$ - or  $\beta$ CD is degraded by the three enzymes. However, it was also reported that after 24 hours of incubation with the amylase about 20 % of the initial  $\beta$ -CD concentration was hydrolysed by PPA while HSA seemed incapable of any degradation of  $\beta$ -CD even after 42 hours of incubation at very high enzyme concentrations. The main product of the hydrolysis was shown to be maltose while tetraose and the larger sugars were not present.

Marshall & Miwa (1991) used the pancreatic enzymes and showed a larger affinity towards  $\gamma$ -CD than amylase from saliva, although the kinetic parameters of HSA were not mentioned. The  $K_M$  values were reported to be 0.8 mM for HPA and 0.97 mM for PPA,  $V_{max}$  values were not given. Once again the mode of action was shown to be multiple attacks, but with the elaboration that the opening of the cyclodextrin ring was discovered as the rate-limiting step. Finally, Kondo and co-workers demonstrated that all CDs may act as competitive inhibitors of the hydrolysis of pentose (Kondo *et al.*, 1990).

The different kinetic parameters for the hydrolysis of  $\gamma$ -CD by  $\alpha$ -amylase reported in the above mentioned works are listed in table 1:

**Table 1: Overview of the enzymes used, the kinetic parameters, and experimental conditions in available publications.**

Enzyme	Enzyme amount	$K_m$	$V_{max}$	pH	Reference
<i>A. oryzae</i>	1.62 $\mu$ M	3.12 $\mu$ M	2300 $\text{min}^{-1}$	5.2	Jodal <i>et al.</i> (1984a+b)
Porcine pancreatic	50 nM	0.97 mM	-	6.9	Kondo <i>et al.</i> (1990)
Human pancreatic	50 nM	0.8 mM	-	7.0	Kondo <i>et al.</i> (1990)
	58 mU/ml	2.9 mg/ml	1.1 $\mu$ g/30 min/mU	5.3	Marshall & Miwa (1981)
	72 mU/ml	4.7 mg/ml	0.32 $\mu$ g/30 min/mU	6.9	
Human salivary	114 mU/ml	5.3 mg/ml	0.3 $\mu$ g/30 min/mU	5.3	Marshall & Miwa (1981)
	166 mU/ml	7.1 mg/ml	0.21 $\mu$ g/30 min/mU	6.9	

As seen from the table the different results reported in the publications are difficult to compare directly as the experimental conditions vary and different units of amylase have been used. This means that a clear overview of the degradation by  $\alpha$ -amylase and how the presence of a complexed guest affects the degradation remains unexplored.

The complexation between hydrophobic compounds and CDs serves various purposes and is exploited in many different industries. The cavity may shield the guest from the surroundings thus improving the stability by protecting the compound against degradation by heat, light and/or oxidation. *In vitro* heat degradation of penicillin G has been shown to be nine times slower when the drug was complexed with hydroxypropyl  $\beta$ -CD (HP $\beta$ -CD) than without the CD (Ong *et al.*, 1997). Thymopentin is an immunostimulant so hydrolytically unstable that it loses activity within one week, but when complexed with HP $\beta$ -CD the activity is maintained for more than a year at 25°C (Brown *et al.*, 1993). In the food industry it is possible to use  $\beta$ -CDs to delay browning by several hours by complexing the substrate of an oxidase whose products are the causes of browning – without  $\beta$ -CD browning occurs within minutes (Hicks *et al.*, 1996). Other uses are: masking unwanted odour and/or smell, removal of cholesterol or fatty acids, and so on (Hedges, 1998). In the pharmaceutical industry, the effects exploited include: half-lives are prolonged, unstable drugs become storable, improvement of the organoleptic properties of a bad-tasting compound etc. But one of the most important applications may be the effect on solubility and on the dissolution rate that CDs have on hydrophobic drugs. This effect is used by the pharmaceutical industry in the process of discovering and generating new drugs and in the formulation of poorly soluble drugs.

Lipinski (2000) described two different approaches towards drug discovery. One is the traditional high-throughput screen (HTS) in which leads, that target a specific receptor, are discovered on the basis of screens of thousands of different potential compounds. The other approach, “rational drug design” (RDD), is not based on empirical *in vitro* studies, as opposed to HTS, but on a more rational approach like, for instance, modifications of already known compounds or designing a drug based on existing information on the target site in question. The problem of the two approaches is that the leads generated tend towards lower permeability or lower aqueous solubility. When searching for leads using HTS one tends to get more hydrophobic results since this feature generally will result in a better receptor affinity *in vitro*. With RDD the number of hydrogen bonds will increase, for instance, due to

an attempt to increase binding affinity via hydrogen bonds. RDD and HTS share a common feature, in spite of their very different approaches, which is a trend of higher molecular weight during time (Lipinski, 2000), as seen on figure 2.

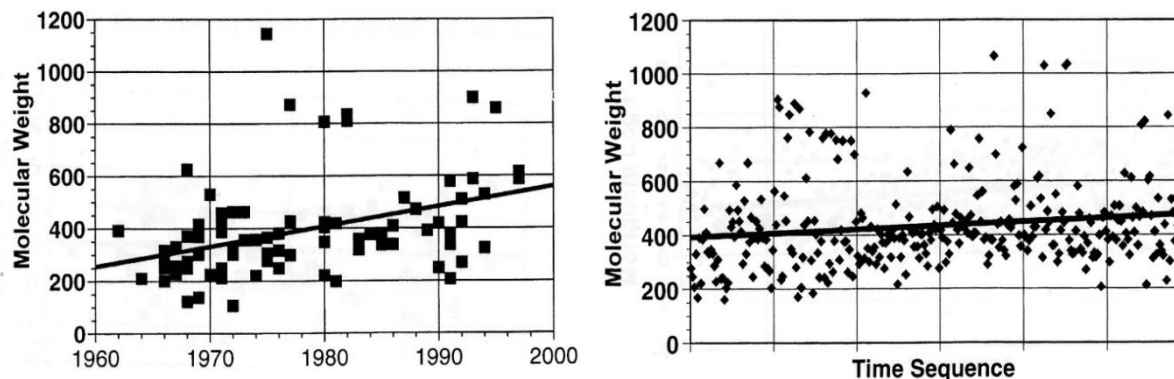


Figure 2: The figure illustrates the trend towards higher molecular weight in time of the drug candidates of Merck (left) and Pfizer (right). The points in the Pfizer curve represent candidates in a much earlier state than the Merck candidates which is the only reason to the apparent larger amount of Pfizer candidates compared to Merck candidates. The time sequence in the Pfizer curve is approximately the same as the Merck time sequence. Figure from Lipinski (2000).

The problems mentioned above are linked together in Lipinski's rule of five. This is a guideline based on computational analysis of 2245 compounds. It states that poor absorption and permeability is more likely when there are more than five hydrogen bond donors and more than 10 hydrogen acceptors, the molecular weight is above 500 Da and logP is above 5 (Lipinski *et al.*, 1997). This indicates that the problem with increased molecular weight, hydrogen bonding, and hydrophobicity (expressed by logP) of the HTS and RDD approaches leads to poor biopharmaceutical properties of the compounds, i.e. decreasing and more variable bioavailability from traditional pharmaceutical formulations. Absorption and thereby bioavailability are directly linked to permeability and aqueous solubility when it comes to oral drug formulations – figure 3 illustrates this connection.

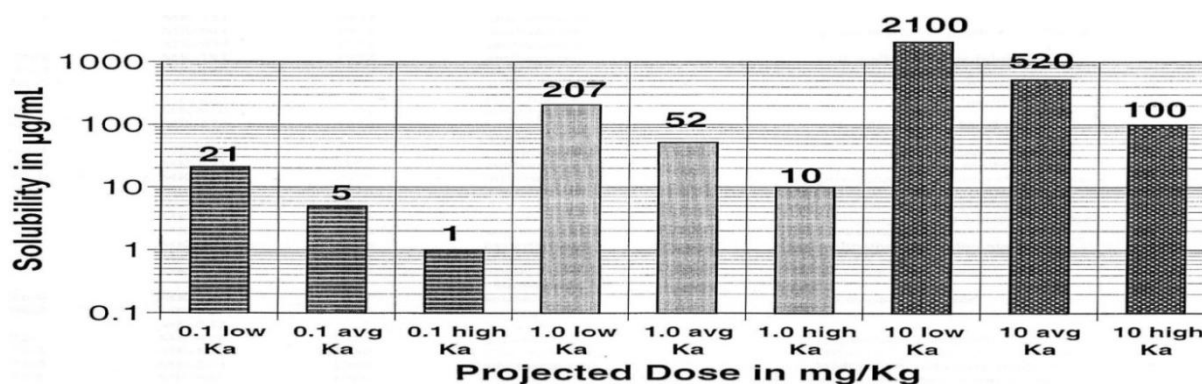
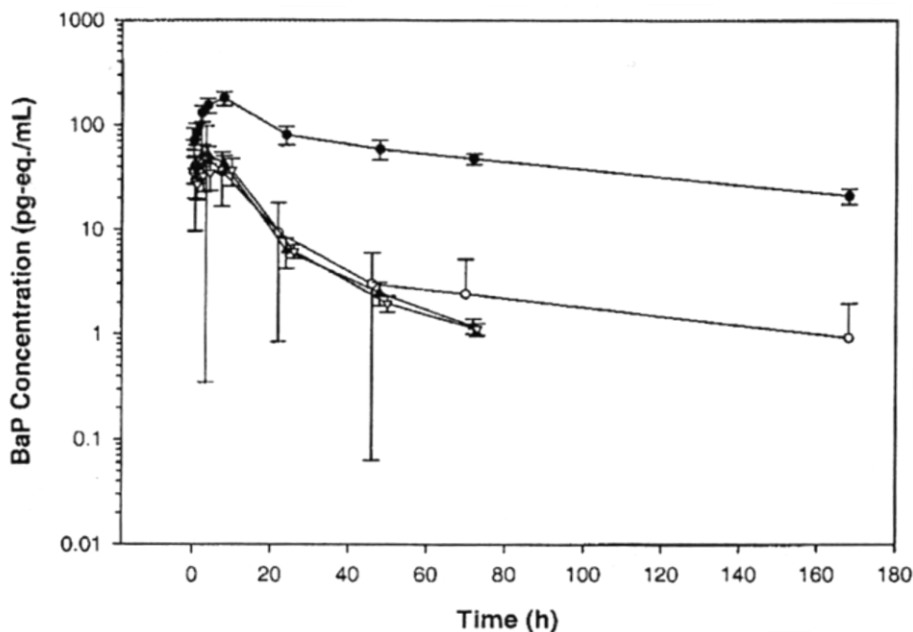


Figure 3: The figure shows three sets of bars representing three different oral administrations of, from left to right, 0.1 mg drug/kg body weight, 1.0 mg drug/kg body weight, and 10 mg drug/kg body weight. Each bar in each set represents a drug with low, average, and high permeability, again from left to right. Figure from Lipinski (2000).

The three sets of bars represent three different oral administrations of, from left to right, 0.1 mg drug/kg body weight, 1.0 mg drug/kg body weight, and 10 mg drug/kg body weight and each bar in each set represents a drug with low, average, and high permeability, respectively. The minimum required aqueous solubility of a drug, in order to avoid poor absorption, is then read off the y-axis. For instance, a drug of low permeability that is administered orally at a dose of 1.0 mg drug/kg body weight (the first bar of the middle set) will need to have an aqueous solubility of 207  $\mu\text{g/ml}$  (Lipinski, 2000) – in comparison, the active ingredient in some analgesics, flurbiprofen, has been shown to have a solubility of 10  $\mu\text{g/ml}$  at pH 6.3 and 25 °C (Li & Zhao, 2003). Since the tendency of new drugs and drug candidates, as already stated, is that they are more and more hydrophobic the concomitant lacking solubility is a problem and not only concerning absorption in humans. When the *in vitro* screens, be it HTS or RDD, result in a candidate the next step is to identify the physico-chemical properties and to determine the pharmacokinetic and pharmacodynamic profiles, i.e. determining adsorption, distribution, metabolism, and excretion, the so-called ADME parameters, *in vivo*.

If a candidate fails these preliminary studies it will be discarded long before human trials are even considered. The failure is often due to the mentioned solubility problems and the consequences that follow: if the compound is poorly absorbed in the animal, ADME cannot be investigated properly and the compound cannot be used. A solution to this problem may be to exploit the ability of the CDs to form complexes with hydrophobic compounds thus increasing their solubility and thereby render ADME experiments possible on otherwise discarded compounds. There are quite a few reviews on the use of cyclodextrins as carriers in the mentioned early animal experiments but most of them deal mainly with the use of  $\beta$ -CD and modifications of  $\beta$ -CD (Maas *et al.*, 2007; Uekama *et al.*, 1998; Uekama, 2004). The reason for this more extensive use of  $\beta$ -CD is partly historical, and partly due to the fact that  $\beta$ -CD generally forms more stable complexes than  $\gamma$ -CD with most drug candidates. Still,  $\gamma$ -CD has the advantage of size and thereby more likely to be able to form complexes with the larger compounds that seems to be the standard of new drugs. Also,  $\gamma$ -CD is, as mentioned earlier, more water soluble. Furthermore, two Swedish researchers have described another problem with  $\beta$ -CD. They found that when dosing  $\beta$ -CD to rats orally with increasing amounts of CD the bioavailability of the concomitant dosed benzo[*a*]pyrene *decreased*. They hypothesized that the complex association was so strong that it reduced the available amount of free benzo[*a*]pyrene in the intestine and thereby the bioavailability, as the complex cannot

be absorbed (Westerberg & Wiklund, 2005). One can imagine that when the complex affinity is high, the drug will be included in an “empty” CD as soon as it is released from its host. This will shift the equilibrium between the drug in complex and the drug in solution towards the complex, thus leaving a smaller amount of free solubilised drug than if the drug had been administered without CD, as illustrated on figure 4.



**Figure 4:** The figure shows the concentration of benzo[a]pyrene in rat plasma during time with and without the addition of  $\beta$ -CD. The top curve is without any CD addition while the curves below illustrates the addition of more and more CD. Figure from Westerberg & Wiklund (2005).

$\gamma$ -CD is, as mentioned above, a substrate to  $\alpha$ -amylase, as opposed to  $\beta$ -CD, and  $\alpha$ -CD for that matter, which does not seem to be degraded by the amylases in the intestines, or at least only in a very slow manner. That means that instead of shifting the equilibrium towards the complexed form of the drug as in the case with  $\beta$ -CD, the equilibrium ought to be shifted towards the opposite direction since the “empty”  $\gamma$ -CDs will be degraded. Hence, there is a possibility that if  $\gamma$ -CD is used as a carrier the situation with retarding absorption will not occur.

Since  $\alpha$ -CD is not degraded in the intestine it can be considered as a dietary fiber and, in recent years it has been marketed as such and used as a weight loss supplement in USA (Mirafit fbcx®, Alpha-Fibe®) with the argument that it interacts with the dietary fats (Artiss *et al.*, 2006). That is not unlikely since  $\alpha$ -CD has previously been reported to form inclusion complexes with fatty acids (Regiert, 2007). However, Artiss *et al.* (2006) stated that a complex formed between  $\alpha$ -CD and the fats with the ratio 1:9. This ratio was based on the comparison between the amount of fat fed to rats and the amount of fat gained which led to the conclusion that 1 g  $\alpha$ -CD prevented the absorption of 9 g fat. The conclusion was verified

by an *in vitro* experiment in which a large excess of  $\alpha$ -CD was added to a mixture of olive oil and water. The bases of the conclusions, i.e. the calculations and the exact results used for these, were not shown. First of all, the true stoichiometry of the proposed complex must be a lot higher than 1:9 based on the molecular mass of fats (for instance: oleic acid has a mass of 282.34 g/mol, giving a stoichiometry of 1:31). Second, the presence of a complex was never verified and the nature of a complex capable of including, for instance 31 moles of fat pr. 1 mole  $\alpha$ -CD is quite intriguing. It seems more likely, that the weight loss reported by Artiss *et al.* (2006) is not only based in the exclusion of fat. Based on the results from Kondo *et al.* (1990) it may be hypothesised that the due to  $\alpha$ -CD capability of inhibiting the hydrolysis of starch and the calorie uptake will thereby be reduced. A connection between low glycaemic index diets and weight loss/maintenance has been shown (Ludwig, 2003) and investigations have shown that on addition of  $\alpha$ -CD to a carbohydrate-rich meal, the glycaemic response is reduced. These results indicate that  $\alpha$ -CD does, in fact, inhibit the amylases of the intestine but it may also be related to the retention time of the intestine: if the fluid volume of the intestine is increased, for instance due to osmotic pressure caused by the hydrophilicity of  $\alpha$ -CD and accumulation of starch attributable to the proposed inhibitory effect on amylase, the retention time would be retarded and as such the time available for starch degradation and glucose absorption (Buckley *et al.*, 2006).

The effect of the addition of  $\alpha$ -CD on the degradation of  $\gamma$ -CD has not yet been shown.

The above considerations lead to the following problem statement of this thesis:

## 1.1 Problem statement

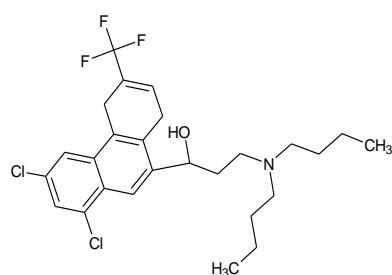
It has been shown that  $\beta$ -CD, when administered in excess orally, may decrease the bioavailability of a hydrophobic drug, most likely due to profound complexation.  $\gamma$ -CD is a substrate to  $\alpha$ -amylase and should therefore be degraded at a reasonable rate unlike  $\alpha$ -CD and  $\beta$ -CD which only to a limited extent, if at all, are degraded. The hypothesis is that  $\gamma$ -CD is a better carrier for hydrophobic molecules that are to be tested in the early animal experiments since the situation with a decrease in bioavailability should not occur due to the degradation. The questions to be answered are therefore if or how the release of drugs from  $\gamma$ -CD is affected by the amylase degradation and whether complex stability has any influence on this. Additionally, the effect of adding various concentrations of  $\alpha$ -CD to a solution of  $\gamma$ -CD and  $\alpha$ -amylase will be investigated.



## 2 Experimental aspects

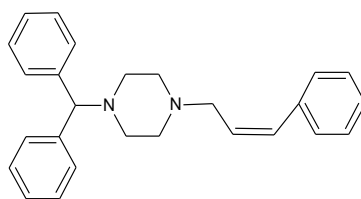
The stability constant and stoichiometry of 6 different  $\gamma$ -CD complexes are to be determined. The degradation of CDs, both native and their hydroxypropyl derivatives, by  $\alpha$ -amylase will be investigated in detail using amylases from various origins. The effect of a mix of cyclodextrins on the degradation will be investigated using porcine  $\alpha$ -amylase. Two complexes with relatively small and large complex stability constants will be chosen and the *in vitro* degradation by porcine  $\alpha$ -amylase of each will be investigated.

Six compounds have been selected on the basis of their various hydrophobicities and their known ability to form inclusion complexes with  $\gamma$ -CD: ibuprofen (IBU), flurbiprofen (FLU), danazol (DAN), cinnarizine (CIN), benzo[*a*]pyrene (BEN), and halofantrine (HAL). The molecular structures as well as relevant data of all six compounds are shown on figure 5.



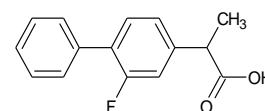
**Halofantrine**\*

Mw: 500.4 g/mol  
logD<sup>†</sup>: 5.6 (pH 7)  
pK<sub>a</sub>: 10.2



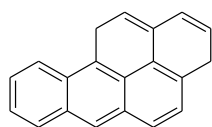
**Cinnarizine**\*

Mw: 368.514 g/mol  
logD<sup>‡</sup>: 4.5  
pK<sub>a</sub>: 1.95  $\wedge$  7.5



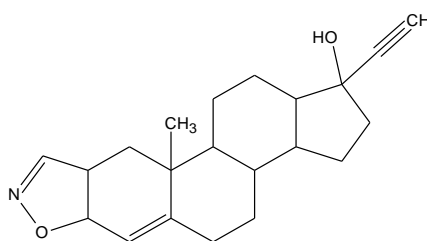
**Flurbiprofen**<sup>‡</sup>

Mw: 244.261 g/mol  
logD<sup>§</sup>: ~-0.9 (pH 7.4)  
pK<sub>a</sub>: 4.2



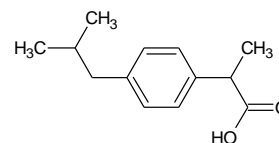
**Benzo[*a*]pyrene**<sup>#</sup>

Mw: 252.31 g/mol  
logP: 6.2  
pK<sub>a</sub>: -



**Danazol**\*

Mw: 337.5 g/mol  
logD<sup>‡</sup>: 4.57  
pK<sub>a</sub>: 13.1



**Ibuprofen**<sup>±</sup>

Mw: 206.281 g/mol  
logD<sup>±</sup>: ~2  
pK<sub>a</sub>: 4.8

**Figure 5:** The molecular structure of the compounds to be used including relevant physical constants. \* Kaukonen *et al.* (2004), except the pK<sub>a</sub> value of halofantrine which was determined by E. Jørgensen, H. Lundbeck A/S; <sup>‡</sup> Wishart *et al.* (2008); <sup>#</sup> Haynes (2010); <sup>†</sup> PubChemCompound (2010); <sup>‡</sup> Fagerberg *et al.* (2010); <sup>§</sup> Ito *et al.* (2007); <sup>±</sup> Hadgraft & Valenta (2000).

Reaction medium will be a 50 mM TRIS-maleate buffer as described by Zangenberg *et al.* (2001), though a 50 mM phosphate buffer will be used for the solubility experiments. pH of the buffers will be 6.5 in order to mimic the environment of the small intestine. At this pH all compounds but BEN will be charged: IBU and FLU will be deprotonised, hence have a negative charge although approx. 1 % will be protonised, while HAL and DAN will be protonised and have a positive charge. One of the nitrogen atoms of CIN will be fully deprotonised while approx. 10 % of the molecules will have the other nitrogen atom deprotonised. The logD value of HAL and FLU are valid at higher pH values than 6.5. This is not of importance in the case of HAL since it will be fully protonised at both pH values. It will, though, make a difference with FLU since it must be considered fully deprotonised at pH 7.4 but not, as mentioned above, at pH 6.5. Due to the similarities between IBU and FLU the logD of FLU is most likely of the same magnitude as that of IBU. The logD values of IBU and FLU is read from a graph, hence the stated approximation.

## 2.1 Characterization of inclusion complexes

A complex between CDs and a guest can be characterised by the stoichiometry of the complex and its stability constant – and the former is compulsory in order to determine the latter. Stoichiometry of the complex can be determined with Job's plot, also called the method of continuous variation. The setup for the plot is based on two stock solutions of equal concentrations of guest and host. A mixture is made with gradually increasing mole fraction of the host and an observable parameter of complex formation is measured. These data are plotted as a product of the mole fraction of the guest against the mole fraction of the host and stoichiometry can be interpreted from the maximum, as illustrated on figure 6, with the only condition that only one type of complex is present in the mixture (Fielding, 2000). However, the method most often used is simple conjecture, albeit qualified,

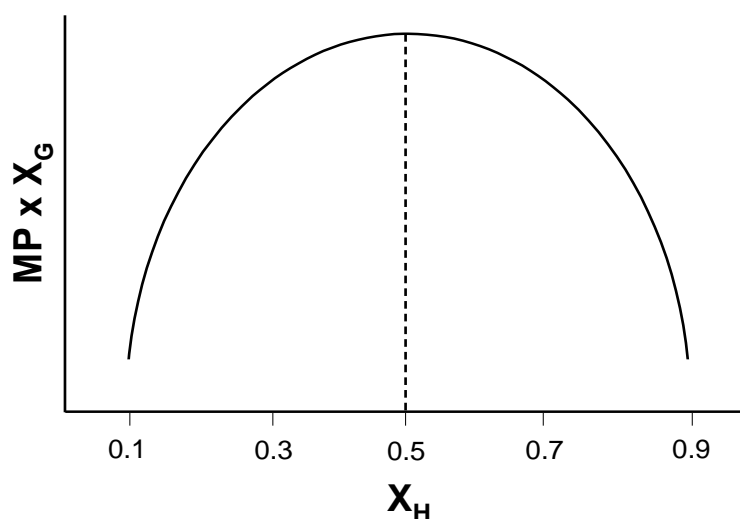


Figure 6: The figure is a sketched image of Job's plot. The mole fraction of cyclodextrin is shown on the x-axis while the product between the measurable parameter (MP) and the mole fraction of the guest is shown on the y-axis.

based on structure of the guest(s) followed by tests of consistency or lack thereof – for instance, comparison between calculated stability constants at various concentrations and/or determined from different methods. These methods may roughly be divided into two types depending of their approach: solubility diagrams and methods, based on shifts in a measurable parameter due to the complexation. The latter covers a very broad spectrum of analytical methods: absorption spectroscopy, calorimetry, nuclear magnetic resonance (NMR), electrophoresis, and many more (Connors, 1996). Of these three methods, solubility diagrams, NMR, and affinity capillary electrophoresis (ACE), seems immediate available to the project. The Higuchi-Connors phase-solubility diagrams are solubility diagrams with the advantages of a simple setup, simple data analysis, and the fact that it is applicable to all six compounds. Under the prerequisite of ideality, the method generates information on intrinsic solubility of the compounds and solubility, stability constant, and stoichiometry of the complexes meaning that each complex can be characterized in one experiment. For this reason, the method is chosen for the experiments and the theory behind it is described in the following.

The setup consists of a dilution series of ligand concentrations with constant volumes followed by the addition of a considerable excess (compared to its intrinsic solubility) of the insoluble or slightly soluble compound (in the following abbreviated ‘G’ for guest) that are to be complexed to the ligand/ CD.

The suspensions are brought to the solubility equilibrium at a constant temperature before samples are taken for analysis. The idea is that when the excess G is removed, the remaining solution will contain, apart from the added quantities of ligand, only the G in solution – whether it be in free form or

complexed. The assumption is that if the ligand concentration, called H for host, is plotted against the

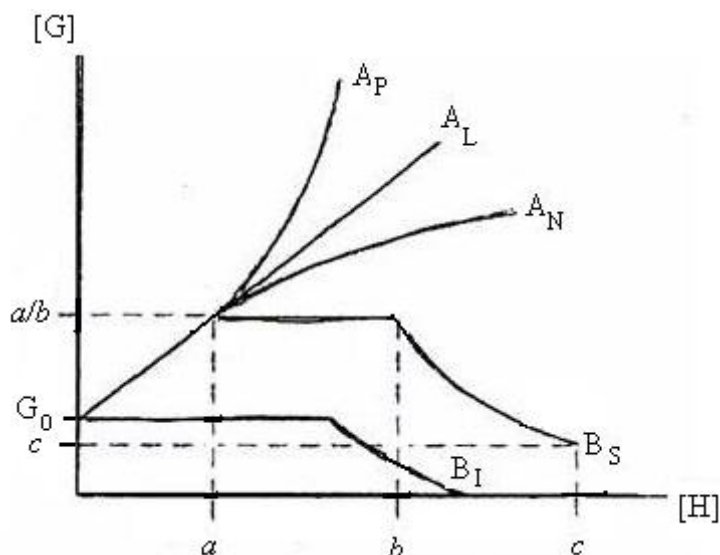


Figure 7: Higuchi-Connors phase solubility diagram showing the diagram of a soluble (A) and insoluble or less soluble (B) complex. [G] is the concentration of the guest, [H] the concentration of the host, and points a, b, and c each represents a distinct development in the solubility isotherm. Figure modified from Higuchi & Connors (1965).

concentration of G found in the solution any increase of G will be due to complex formation between H and G. The intersection with the y-axis will then represent the intrinsic solubility

of  $G$ ,  $G_0$ . Indeed, from such a plot two types of diagrams, A and B, may emerge, see figure 7. Type A diagrams are seen when the obtained complexes are soluble indicating that the ligand has facilitated an increase in the solubility of  $G$ . As seen on the figure three variants of type A diagrams exist: Line  $A_L$  is obtained when the complexes are in first order with respect to the guest – applied to cyclodextrins as “ligands”, that would mean a host-guest ratio of 1:1, 1:2, 1:3 etc. If there is a positive curvature, as seen with  $A_P$ , complexes with a higher order with respect to the ligand (host-guest ratio of 2:1, 3:1, 4:1 etc.) are present. A negative curvature,  $A_N$ , may be seen if  $H$  at large concentrations self-aggregates or if large  $H$  concentrations lead to some alteration that effects the stability constant of the complex (Higuchi & Connors, 1965).

Type B diagrams represent the situation where less soluble or insoluble complexes are formed. Two variants of B exist: If the complexes formed are so insoluble that no increase in solubility of  $G$  can be detected, the result would be line  $B_I$  – the plateau and the decline is also seen in line  $B_S$  and is described there. Line  $B_S$  is similar to  $A_L$  in the beginning of the increase but at a critical concentration of  $H$ , point  $a$ , a plateau emerges indicating a limit in the solubility of the complex, hence, the ordinate,  $G_a$ , is the value of the complex solubility. Point  $b$  will be reached when all solid  $G$  present in the system has been complexed and consequently every complex has precipitated. With no  $G$  on complexed form in the solution the apparent decline in the solubility is seen and this apparent decline will continue until point  $c$  is reached. On the figure, point  $c$  is below  $G_0$  which is a situation that may happen if different types of complexes can occur. In other words, if the complex responsible for the initial rise to point  $a$  is not the same as the complex precipitating along the line from  $b$  to  $c$ , the solubility will drop below the intrinsic value (Higuchi & Connors, 1965).

Besides information on solubility, also stability constants and stoichiometry can be estimated from Higuchi-Connors diagrams. Diagrams of the A type, though, cannot be used to determine the stoichiometry of the complex unless a plateau is present similar to type B. This may happen if  $G$  is completely solubilised or the solution is saturated with respect to  $H$ . In contrast, it is always possible to estimate stoichiometry from type B diagrams if the amount of  $G$  added to the system in total is known and if point  $b$  is reached. This is possible due to the fact that the plateau represents the exact amount of ligand on complexed form and that the amount of  $G$  on complexed form can be calculated by subtracting the amount of  $G$  in solution in point  $a$  from the total amount of added  $G$ , see figure 7 for references. The ratio between

these two amounts is equal to the stoichiometry of the complex. For instance, the total amount of added G is 10 mM and in point *a* 2 mM is solubilised. The amount of H in *b* is 15 mM and in *a* 6 mM. In cyclodextrin terminology this gives the host-guest ratio of  $\frac{15-6}{10-2} = \frac{9}{8} = \frac{1,13}{1}$  which must be presumed to correspond to a ratio 1:1. If the descending part of type B diagrams is a straight line, the stoichiometry can be calculated from this albeit an extrapolation down to the x-axis is necessary (Higuchi & Connors, 1965).

As mentioned, calculation of stability constants requires that the stoichiometry is known. But as the above discussion has shown, it is not always possible to give more than an estimate to the stoichiometry from the diagrams. For this reason, the stability constant calculations are often based on an assumption of a reasonable stoichiometry and the result is therefore somewhat ambiguous. But for this project, the exact value of the stability constant is not as interesting as the relative magnitude between the different complexes and the method would therefore be quite sufficient.

It is expected that the complexes have a relatively low solubility due to the fact that most of the guests will have parts protruding from the cavity that will not promote the solubility particularly. Hence, the assumption must be that a solubility diagram will be of type B which is why stability constant calculations in the following will focus mainly on the B type while calculations based on the other types of diagrams will be addressed only briefly.

Calculations of stability constants from either type of diagram have the usual equilibrium expression as starting point:

$$K = \frac{[G_m H_n]}{[G]^m [H]^n} \quad (1)$$

in which G is the compound to be complexed, H is the ligand (CD) and m and n are the coefficients of G and H, respectively. The components of the fraction are either known, if the stoichiometry is known, or they can be expressed from known values:

$$[G] = G_0 \quad (2)$$

$$[G_m H_n] = \frac{G_t - G_0}{m} \quad (3)$$

$$[H] = H_t - n[G_m H_n] \quad (4)$$

in which  $H_t$  is the total amount of ligand added to the system and  $G_t$  is the total amount of G in solution regardless of phase. With  $n=1$  equations 1-4 combined gives

$$G_t = \frac{mK_{1:m}G_0^m}{1 + K_{1:m}G_0^m}H_t + G_0 \quad (5)$$

which is the equation of an  $A_L$  diagram. This means, that the intercept with the y-axis, as already stated, yields the intrinsic solubility while the fraction yields the slope. More interestingly, equation (5) shows that the stability constant can be calculated from the slope using the following equation:

$$K_{1:m} = \frac{\text{slope}}{G_0^m(m - \text{slope})} \quad (6)$$

Now, in the case of a 1:1 stoichiometry the evident problem is that in the ideal situation a complex of the 1:1 form must result in a slope of exactly 1, and then the above formula is invalid. Also, if the slope is larger than 1, if only by a fraction,  $K_{1:1}$  equals a negative value. However, isolating  $K_{1:m}$  from (5) yields the more complex formula which can be used in the, perhaps rather unlikely, case of a slope of exactly 1 or a slope larger than 1:

$$K_{1:m} = \frac{G_t - G_0}{G_0^m(mH_t - G_t + G_0)} \quad (7)$$

The above two formulas is valid both for  $B_S$  and  $A_L$  diagrams. In the case of an  $A_P$  or  $A_N$  diagram, it is often used to assume 1:1 stoichiometry or to use a linear regression to fit the best line between the data points and then use equation 6. A better estimation, though, is achieved if it is assumed that the  $A_P$  curve arises from a mixture between 1:1, 1:2 and so on, meaning  $K_{1:1} = \frac{[HG]}{[G][H]}$  and  $K_{1:2} = \frac{[HG_2]}{[HG][H]}$  etc., and then base the calculations of the stability constant on the same mass balance equation as above. With  $B_I$  diagrams, and  $B_S$  for that matter, the calculations can be based on the decreasing part of the line using the assumption that the concentration of G and H in any point of the descending part can be expressed as the sum of the concentration of each compound in solution and the concentration of the complex times the relevant coefficient. At point  $c$  on figure 7, all free G has been complexed meaning that complex concentration must be equal to concentration of G in point  $c$ . These reflections lead to the following equation:

$$K_{m:n} = \frac{G_c}{(G_x - mG_c)^m \cdot (H_x - nG_c)^n} \quad (8)$$

in which  $G_x$  and  $H_x$  is the concentration of each compound at any point on the descending part of the curve (Higuchi & Connors, 1965).

### 3 Materials and methods

Suppliers and quality of all chemicals are listed in appendix I. The buffers used were either a 50 mM phosphate buffer, pH 6.5 (buffer A) or a 50 mM TRIS-maleate buffer (buffer B), made from 50 mM TRIS-base, 50 mM maleic acid, 30 mM NaCl, and 4 mM CaCl<sub>2</sub> and adjusted with 4 M NaOH to a pH of 6.5. HP- $\gamma$ -CD was tested for the presence of native  $\gamma$ -CD on a LC-MS (Bruker Esquire LC) – spectrum can be seen in appendix II. Lot numbers and suppliers are listed in appendix I.

#### 3.1 Determination of complex stability constants

A stock solution of suitable concentration of  $\gamma$ -CD was prepared in buffer A. From the stock solution a dilution series was prepared in 4 ml glass vials using buffer A. A few milligrams of relevant drug were added to each vial which was then placed in a sonicator (Covaris S2) for 30 or 100 (DAN, HAL and BEN) seconds. pH was checked and adjusted if necessary with either 2 M NaOH or a 50 % methansulfonic acid solution before sonicating and rechecking pH again. When pH had stabilised the vials were placed in a tumbler at 37 °C and the pH checked regularly and adjusted if necessary. When pH-stabilised (after 1-2 days), or in the case of the neutral DAN and BEN after approx. 48 hours, the solutions were filtrated using preheated syringes and 0.22  $\mu$ m filters (Millex-FG, Millipore Corp., MA, USA) and diluted to an appropriate concentration with mobile phase. The solutions were then analysed on HPLC (Merck Hitachi, 7000-series) equipped with a Waters XBridge<sup>TM</sup> C18 column, DAD detection (Merck Hitachi, 7000-series), and 25 mM phosphate buffer, pH 6.0, and methanol (35/65 v/v%) as mobile phase in the case of IBU, FLU, and DAN. BEN, CIN, and HAL were analysed on with a similar set-up, only using an UV detector (Merck Hitachi, 7000-series). As for BEN the mobile phase was a 15/85 v/v% mix of a 5 mM phosphate buffer, pH 6.0, and acetonitrile and wave length 267 nm, and as for CIN and HAL the mobile phase was a 20/80 v/v% mix of buffer and methanol and wave length 210 nm and 254 nm, respectively. Flowrate was set at 1 ml/min and column temperature was 40 °C. Concentrations were calculated on the basis of the ratio between the area under the curve of the drug signal and the signal of either 0.1 mg/ml or 0.01 mg/ml standard solutions made in mobile phase (IBU), methanol (FLU, DAN, CIN, HAL) or acetonitrile/very little water (BEN). Samples were analysed in duplicates.

### **3.2 Examination of crystal structure of compounds**

In order to check whether the above treatment had caused any structural changes in the compounds, the crystal structure of the precipitate (desiccated left-over of excess compound) was examined using x-ray analysis: after sampling for HPLC analysis as much as possible of the fluid was removed and the vials were left during the night in the incubator for evaporation of fluid and thereby drying of remaining sediment. Diffraction patterns of each compound were then obtained on a PANalytical X'Pert PRO X-Ray Diffractometer (Almelo, Holland) in alpha1 configuration equipped with an X-celerator detector and a crystal graphite monochromator, operated at a voltage of 40 kV and a current of 45 mA. Copper ( $\lambda=1.5406\text{\AA}$ ) was used as anode material and the samples were analysed in the  $2\theta$  angle range of  $5^\circ$  to  $40^\circ$  with step size of  $0.045^\circ$  and a scan step time of 0.5 seconds.

### **3.3 Investigation of degradation of cyclodextrins**

CD solutions were prepared with buffer B and preheated to  $37^\circ\text{C}$ . 2 units/ml of enzyme were added as a solution of enzyme suspended in buffer B, preheated to  $37^\circ\text{C}$  and the vial was placed in a tumbler with slow rotation at  $37^\circ\text{C}$  and the time started. Samples were taken immediately after enzyme addition and at different time points hereafter. The reaction was stopped by heating to  $95^\circ\text{C}$  and analysed for the amount of reducing sugars using the method described by Miller (1959) with a few modifications: 250  $\mu\text{l}$  sample was added to 750  $\mu\text{l}$  of a solution of dinitrosalicylic acid (DNS) consisting of 1 w/v% DNS, 1 w/v% NaOH, 20 w/v% Rochelle salt, and 0.05 w/v% sodium sulphite. The mixture was heated to  $95^\circ\text{C}$  for 15 minutes and then transferred to ice for 20 minutes before being analysed spectrophotometrically at 540 nm using an Eliza reader (Labsystems MultiScan RC). All analyses were performed in triplicates.

### **3.4 Investigation of degradation rates of inclusion complexes**

Complexes were made by adding the relevant drug in excess to a 5 mM CD-solution in buffer B and leave it at  $37^\circ\text{C}$  for 5-6 days. The solutions were then filtrated using preheated syringes and 0.22  $\mu\text{l}$  filters. Enzyme solution was prepared and added as described in section 3.3 and the succeeding sampling, handling, and analysing was carried out as described in the same section.

### **3.5 Influence of $\alpha$ -cyclodextrin on the degradation of $\gamma$ -cyclodextrin**

Solutions with  $\alpha$ -CD and  $\gamma$ -CD in buffer B were mixed to the molar ratio of 1:5, 2:5, 3:5, 4:5, and 5:5, respectively. The experiment was performed as described in section 3.3.



## 4 Results and discussion

In the following sections the results from the experiments will be presented and discussed. As a supplement to this chapter a data disc is enclosed with the report containing all raw data.

### 4.1 Characterization of complexes

Six compounds were selected for complexation with  $\gamma$ -CD based on their hydrophobicity: ibuprofen (IBU), flurbiprofen (FLU), danazol (DAN), cinnarizine (CIN), benzo[*a*]pyrene (BEN), and halofantrine (HAL). The stoichiometry, solubility, and stability constant of each complex as well as the intrinsic solubility of each compound were determined using the Higuchi-Connors solubility diagram.

In order to obtain the diagrams the samples were subjected to ultrasound and in some cases pH adjustment (see section 3.1 for reference). This means that first and foremost it must be verified that this procedure does not cause any alterations to the compounds that could affect the complexation. The precipitate of three compounds, FLU, DAN, and BEN, were therefore analysed using X-ray diffraction, see figure 8, with the purpose of screening for any structural changes. Note, the diffractograms are graphically manipulated in the way that the red curve, representing the reference, is lifted with respect to the blue curve, representing the precipitate, in order to facilitate the comparison of the two. In reality, there is no difference between the baselines. As seen on the figure, the curve of the precipitate shows neither any additional peaks compared to the reference, a sample of the pure and thus untreated compound, nor is there any peak alterations. This means that the compound in the precipitate is the exact same compound as the reference, meaning no signs of any structural alterations were identified nor was any salt formation detected. Since it is considered very unlikely that IBU, CIN, and HAL should get any other result considered they have very similar functional groups as the tested compounds, it was concluded that the treatment during the experimental preparations was harmless to all compounds and thus should have no influence on the complexation and thereby the stability constants.

In the following the diagrams of each complex will be examined starting with that of CD-BEN on figure 9 on page 27.

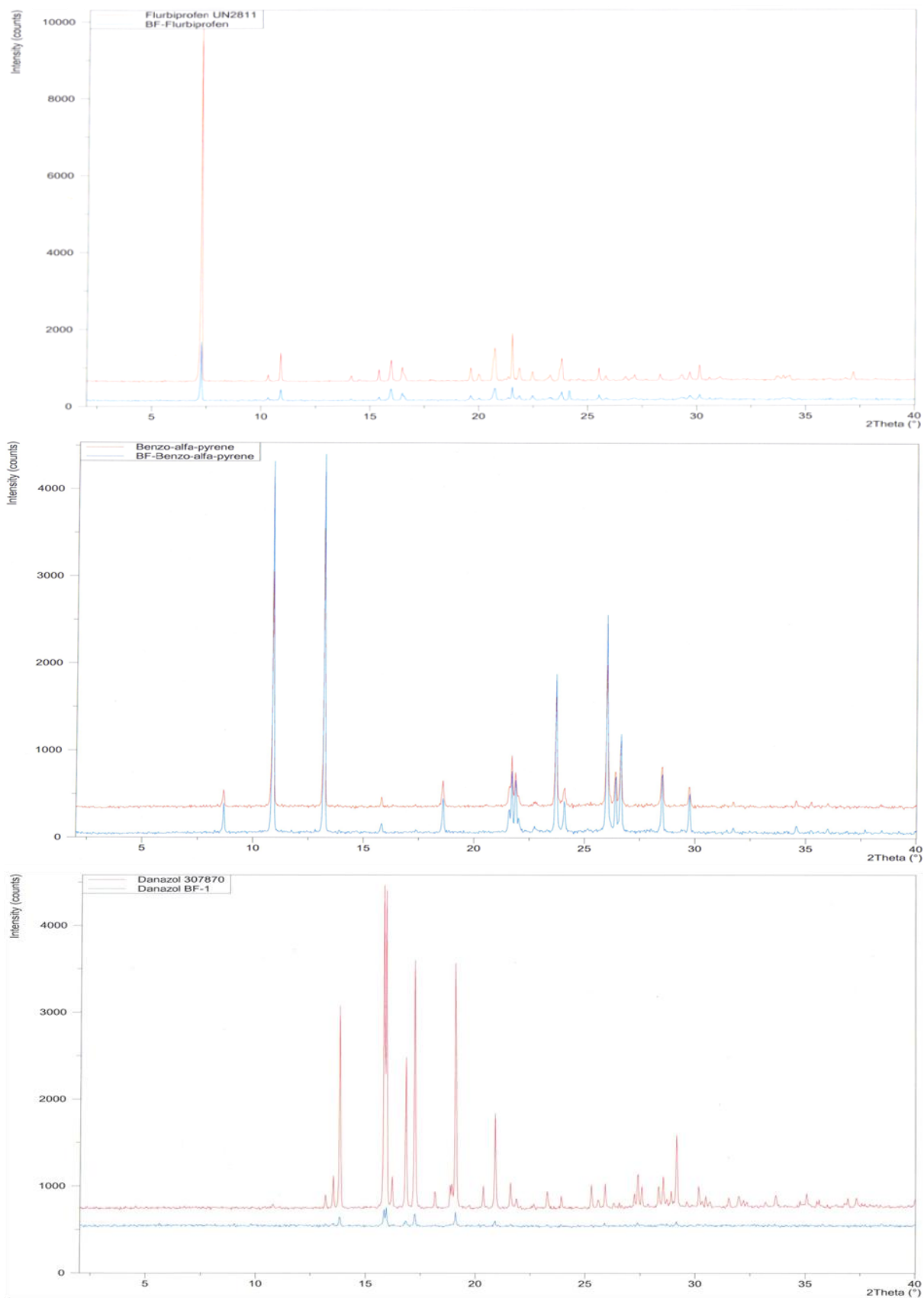


**Figure 8:** The figure shows the comparison between the x-ray analysis of the precipitate (blue) and a sample of the pure and untreated compound (red). The curve of the precipitate has been moved upwards artificially in order to ease the comparison.

#### 4.1.1 The complex between benzo[a]pyrene and $\gamma$ -cyclodextrin

The solubility diagram of the  $\gamma$ -CD-BEN complex, figure 9, is comprised of two individual but identical experiments marked with red and blue, as seen on the left side of the figure. The right side shows the insertion of a trendline so that information on slope and interception point can be obtained in order to calculate the stability constant.

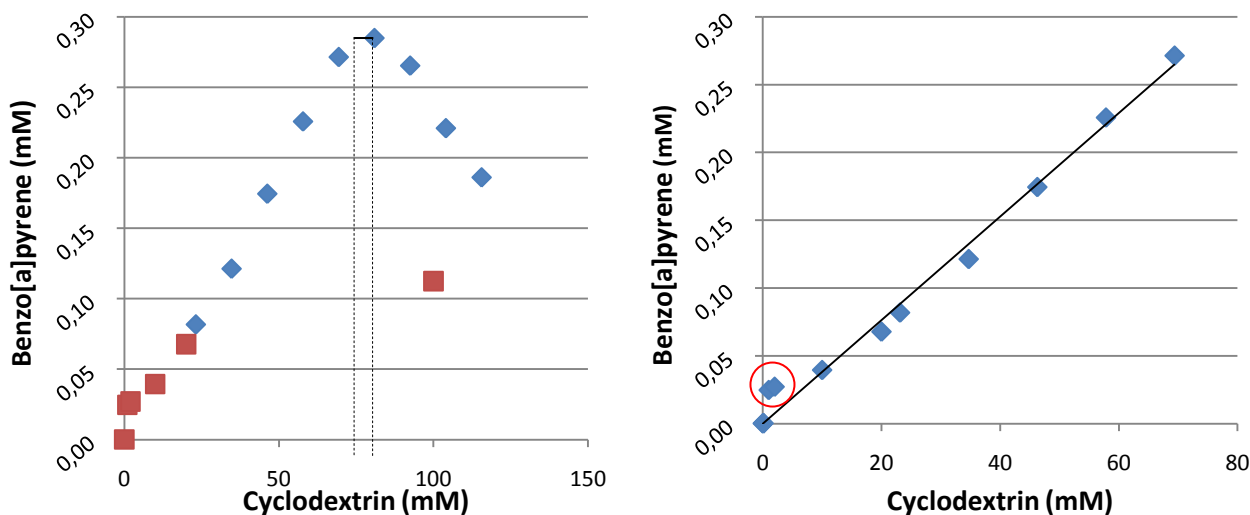


Figure 9: Higuchi-Cornors diagram of the complex between benzo[a]pyrene and  $\gamma$ -cyclodextrin. Left: The graph is comprised of two identical but independent experiments: ■ is the 1<sup>st</sup> experiment, and ♦ the 2<sup>nd</sup> experiment. Right: A trendline is inserted to provide information on slope and intercept.

The first experiment (left figure, red) included a sample comprised of only buffer and BEN as an alternative means of measuring the intrinsic solubility,  $G_0$ . If a trendline through the ascending part of the curves is calculated, the interception of this line with the y-axis would be at  $5.5 \cdot 10^{-6}$  M meaning a  $G_0$  of 5.5  $\mu$ M. However, this is a factor 10,000 larger than the measured  $G_0$  63 nM (see data disc). By comparison, the literature states an aqueous solubility of 17 nM (Haynes, 2010). There is a rather obvious flaw with the use of the trendline to determine  $G_0$ : the determination is very susceptible to outliers further up the line. For instance, the two outliers encircled on the figure to the right pull the line upwards on the y-axis resulting in a larger interception value. This means, that it must be more correct to force the interception point of the trendline with the y-axis to equal the measured  $G_0$ , as it has been done on the right part of figure 9. This results in a line with the equation  $y = 3.7005 \cdot 10^{-3}x + 5.5462 \cdot 10^{-8}$ .

Two things are remarkable on the figure: the outlier in the first experiment (left figure, red) and the lack of an obvious plateau. The former could be caused by lack of BEN in that particular vial but 7.3 mM BEN was added to each vial which is far more than the solubilised amount measured. Another more plausible explanation is some kind of handling or sampling

mistake. The latter must, according to the theory, either be due to a lack of solid BEN meaning that there should have been a further addition of solid BEN in order to create a clearer plateau or be caused by lack of data points in the area. But again, 7.3 mM BEN was added to each vial and the maxima of the curve is 285  $\mu\text{M}$  meaning plenty of BEN has been present at each point of the experiment. According to Higuchi & Connors (see section 2.1) the apparent decline in solubility is caused by the fact that there no longer is solid compound present, but as already stated, plenty of solid benzo[*a*]pyrene were present also at the high CD concentrations. Clearly, this is a situation deviating from the theory but the question is what kind of deviation is the case. If the complexes aggregate it is not unlikely that their solubility diminishes leading to immediate precipitation, which could explain the lacking plateau. Higuchi & Connors actually have an example of a solubility diagram in which the apparent solubility declines from the beginning in spite of excess compound. It was suggested that the phenomenon is caused by the formation of a solid solution. However, first of all it is unknown whether solid solutions can even exist in solutions of molecules. Second, solid solution conditions are described by the Hume-Rothery rules and none of these are met in the present case, which suggests that the presence of a solid solution cannot be the explanation. On the other hand, it has been reported that pure water is able to form a cage-like structure around a hydrophobic compound and still maintain most of the hydrogen bonds thus forming a kind of solid solution (Schmid, 2001). Loftsson *et al.* (2005) proposes that the cage-forming theory might explain some of the deviations observed. However, it is also stated that the theory is valid for pure water as solvent only and the present experiments took place in phosphate buffers. It has not been possible to offer a more satisfying explanation to the phenomenon. The lack of a plateau makes it impossible to calculate the stoichiometry which leaves educated guesses as the only option. A close look on the ascending part shows that there is a very faint tendency towards a positive curvature similar to the  $A_P$  type of diagrams (see figure 7). However, this is clearly not an A-type diagram and since  $A_P$  diagrams indicates host-guest ratios of higher order with respect to CD it seems more likely that the curvature is caused by some systematic error during sampling. On the other hand, a stoichiometry of higher order with respect to CD might be unlikely, since BEN is a relatively small molecule. An estimate of the size of a molecule can be obtained from the software ChemSketch (freeware version, product version 12.01). The length of BEN is estimated to 9.5 Å and the height of the CD torus is 7.8 Å (see figure 1C) which means that parts of the molecule is outside the cavity,

although only a few percent. However, CD aggregations are known to happen and it could be the cause of the curvature. A 1:2 complex has been reported determined by circular dichroism and in the same publication it was mentioned that results showing 2:1 and 2:2 would be published soon thereafter (Kobayashi *et al.*, 1982); it has not been possible to find the mentioned publication, nor to find any stability constants related to the mentioned stoichiometry. Blyshak *et al.* (1989) used dynamic coupled-column liquid chromatography to determine the stability constant of a  $\gamma$ -CD-BEN complex at 35 °C and absorption measurements to determine the stoichiometry. The results were a 1:1 complex with stability constants of 36,510-37,940  $M^{-1}$ . The dimensions of BEN were estimated to 7.1 x 10.4 Å based on standard bond length. It is assumed that the measurements refer to width and length visualizing the molecule in 2D as depicted on figure 5 but knowing the depth would be even more interesting as this would facilitate the stoichiometry reflections. But if 1:1 stoichiometry is assumed to be the case with the present complex, equation (6) yields a constant of 61,240  $M^{-1}$ . The binding energies of this result and that calculated from the results of Blyshak *et al.* (1989) are within the same magnitude rendering the obtained stability constant plausible.

#### 4.1.2 The complex between cinnarizine and $\gamma$ -cyclodextrin

The solubility diagram of the complex between  $\gamma$ -CD and CIN, figure 10, is constructed from a single experiment. The graph on the right shows the insertion of a trendline with the equation  $y = 7.416 \cdot 10^{-4}x - 9.306 \cdot 10^{-3}$ , calculated from the ascending part of the diagram, as well as a line indicating a plateau, calculated from the average value of the five data points, encircled in red, comprising the plateau. A few tendencies can be seen from the diagram.

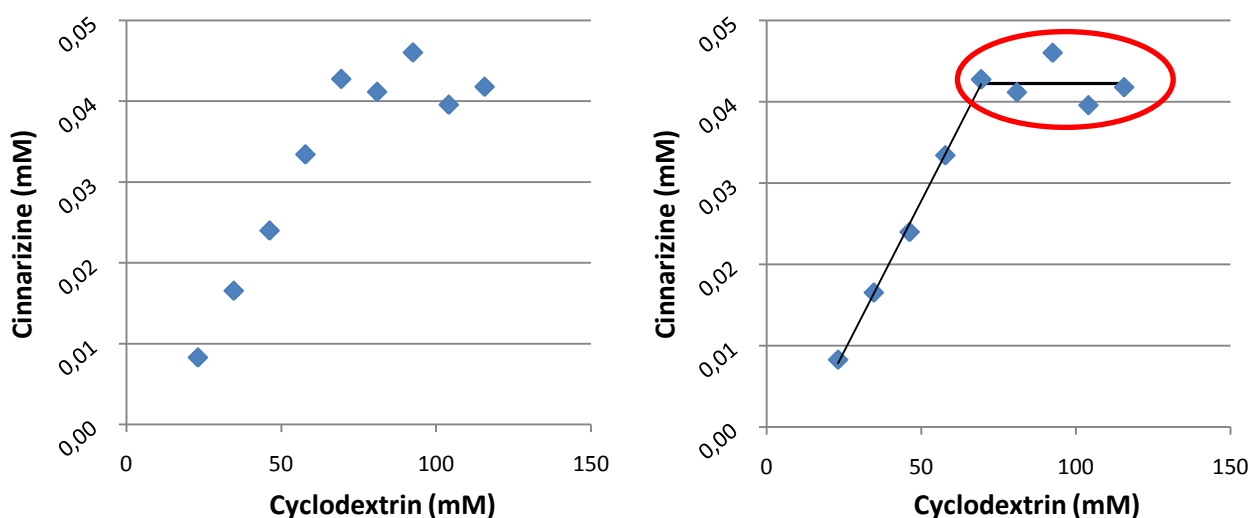


Figure 10: Higuchi-Conners diagram of the complex between cinnarizine and  $\gamma$ -cyclodextrin. Left: The graph is constructed from a single experiment. Right: A trendline is inserted to provide information on slope and intercept. The line indicating the plateau is calculated as the average of the five points comprising the plateau.

As opposed to the CD-BEN diagram, a plateau was clearly observed, however, no descending part occurred in the concentration range used. The CD concentration at the end point is 116 mM. As mentioned in chapter 1 the aqueous solubility of  $\gamma$ -CD at 25 °C is 23.2 g/100 ml equivalent of 179 mM. It has not been possible to find information on the solubility at 37 °C but higher temperature should only increase the solubility. In spite of heavy sonication, agitation, heating, time, etc., it was not possible to dissolve more than the 116 mM which is the reason why the experiment did not go beyond this concentration. There were still surplus CIN present in the 116 mM vial and it is therefore possible that the decline of the curve, as predicted by the theory, could have been reached had a lesser amount of compound been added or had more CD been dissolved. Time issues prevented a repetition of the experiment that could have verified this idea. The absence of the decline, and thus the end point of the plateau, makes it impossible to calculate the stoichiometry and since the slope does not offer any clues either it was not possible to calculate a stoichiometry. As was the case of the CD-BEN complex, no results have indicated a stoichiometry of a higher order, neither with respect to the  $\gamma$ -CD nor to the compound. 2:1 stoichiometries have been reported for complexes with  $\beta$ -CD (Tokumura *et al.*, 1984a; Ueda *et al.*, 1989) with stability constants of  $39.7 \text{ M}^{-1}$  and  $6200 \text{ M}^{-1}$ , respectively. 1:1 stoichiometry for the  $\gamma$ -CD-CIN complex has been reported (Tokumura *et al.*, 1984b) but no stability constant has been found. Since 1:2 stoichiometry and higher are deemed unlikely due to van der Waal repulsion forces the stoichiometry is assumed to be 1:1.

The CD-CIN diagram has another quite peculiar feature: the interception with the y-axis is negative. However, Loftsson *et al.* (2005) has observed this feature too, also with CIN, and it was speculated to have something to do with the high lipophilicity and the structure of CIN. These two characteristics are believed to promote self-association which should be the cause of the negative interception (Loftsson *et al.*, 2005). A sample without added CD was not measured, meaning that no value of  $G_0$  is available other than the negative value. The literature states a solubility in aqueous buffer, pH 7.5 and 37 °C, of 0.1  $\mu\text{g/ml}$  or 0.271  $\mu\text{M}$  (Kaukonen *et al.*, 2004). Using this value as  $G_0$  and the slope mentioned above the stability constant can be calculated to  $2735 \text{ M}^{-1}$ .

#### 4.1.3 The complex between danazol and $\gamma$ -cyclodextrin

The CD-DAN diagram, figure 11, is composed of three experiments, performed independently, marked on the graph to the left with green, red, and blue corresponding to the

first, second, and third experiment, respectively. A good reproducibility can be seen a part from the data points encircled in red on the left figure. The concentrations of danazol measured in the first two experiments are identical (1.03 mM) but in the third experiment the concentration is measured to be approx. 20 % higher (1.23 mM). The data point is most likely the result of a handling or sampling error and the data point was therefore eliminated from the trendline on the right side figure. As with the diagram of CD-BEN, figure 9, the plateau is either lacking or very narrow even though surplus of DAN was still present. That means that conjecture once again is the only option to stoichiometry determination. DAN is a very bulky molecule but does have protruding parts due to its length of approx. 16 Å.

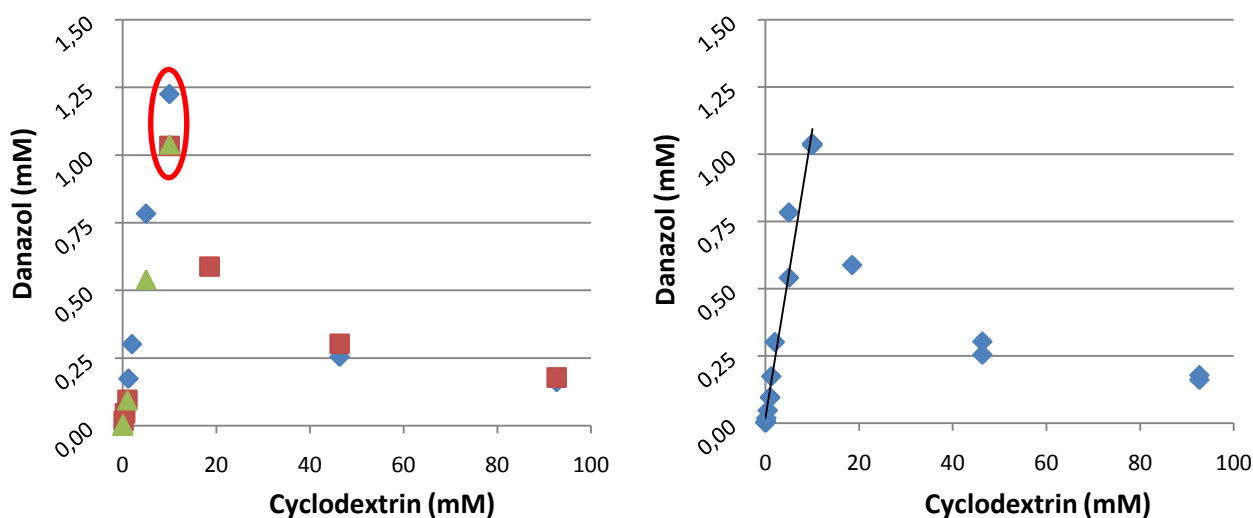


**Figure 11: Higuchi-Corrors diagram of the complex between danazol and  $\gamma$ -cyclodextrin. Left: The graph is comprised of three identical but independent experiments:  $\blacktriangle$  is the 1<sup>st</sup> experiment,  $\blacksquare$  is the 2<sup>nd</sup> experiment, and  $\blacklozenge$  the 3<sup>rd</sup> experiment. Right: A trendline is inserted to provide information on slope and intercept.**

With the nitrogen atom protonised ( $pK_a$  of DAN is 13.1) and hydroxyl group at the opposite end of the molecule it is likely that both ends are protruding from the CD cavity. Both ends have the ability to hydrogen bond with water which is energetically more favourable than complex formation with further CDs. For these reasons the stoichiometry is assumed to be 1:1. The equation of the trendline is  $y = 0.1076x + 1.7965 \cdot 10^{-5}$  giving a  $G_0$  value of 18  $\mu\text{M}$ . This is almost 8 times the amount in the literature of 2.37  $\mu\text{M}$ , achieved with an aqueous buffer, pH 7.5, at 37 °C (Kaukonen *et al.*, 2004). A CD-free sample was prepared in the second experiment and analysed on the HPLC but no distinct peak could be obtained meaning that the concentration of the compound in the sample was below the detection limit. This may be due to the fact that using a DAD detector has the disadvantage of poor sensitivity meaning that concentrations as low as a few  $\mu\text{M}$  has the risk of being consumed by noise. On the other hand, peaks representing a concentration of approx. 1  $\mu\text{M}$  were found in the first experiment.

There is, though, still the possibility that the signal/noise ratio has been different in the two experiments thus explaining the missing signal in one but not in the other. Nevertheless, the question remains whether or not the  $G_0$  from the diagram can be used in the calculations or not. If the  $2.37 \mu\text{M}$  are used the stability constant obtained is  $50855 \text{ M}^{-1}$  while using the  $18 \mu\text{M}$  value results in a stability constant of  $6709 \text{ M}^{-1}$ . Holm *et al.* (2008) analysed, amongst other things, the stability constants of complexes between  $\gamma$ -CD and bile salts using affinity capillary electrophoresis. The stability constants were measured of a complex between  $\gamma$ -CD and taurodeoxycholic acid, a bile salt very similar in structure to DAN, of  $28.000 \text{ M}^{-1} \pm 2700$  with literature values between  $2600 \text{ M}^{-1}$  and  $16000 \text{ M}^{-1}$ . It has not been possible to find any literature values of a  $\gamma$ -CD-DAN complex.  $\beta$ -CD-DAN complexes have been reported, for instance, Jadhav & Vavia (2008) reported a stability constant for a  $\beta$ -CD-DAN complex of  $972.03 \text{ M}^{-1}$  based on 1:1 stoichiometry and calculated from Higuchi-Connors diagrams.

#### 4.1.4 The complex between flurbiprofen and $\gamma$ -cyclodextrin

The diagram is comprised by four identical but independent experiments marked on the graph to the left with purple, green, red, and blue corresponding to the first, second, third, and fourth experiment, respectively, as shown on figure 12. The first experiment consisted of only five different CD concentrations at low CD concentration.

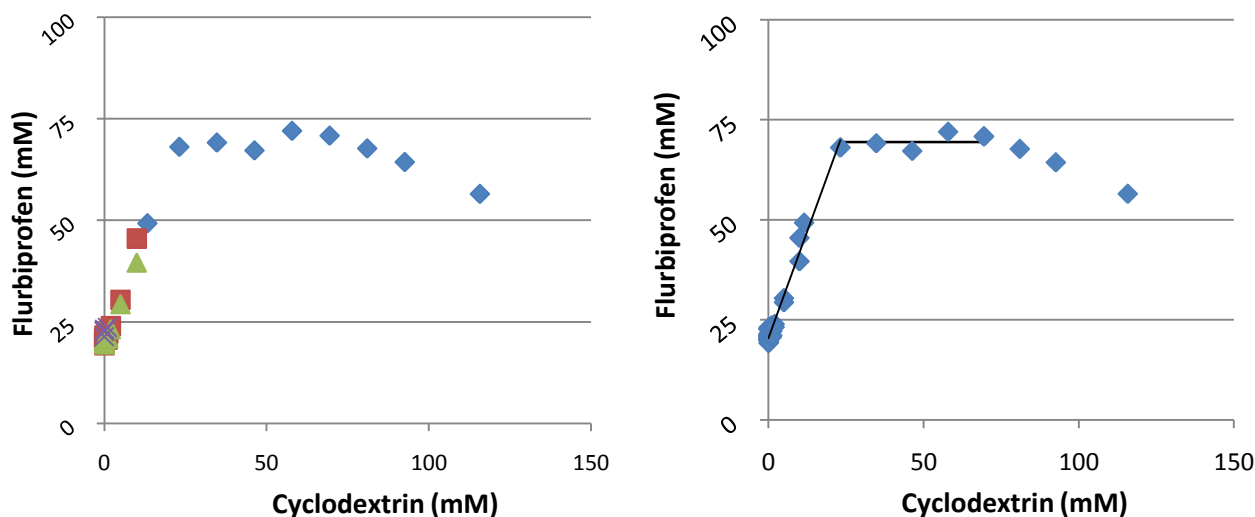


Figure 12: Higuchi-Connors diagram of the complex between flurbiprofen and  $\gamma$ -cyclodextrin. Left: The graph is comprised of four identical but independent experiments:  $\times$  is the 1<sup>st</sup> experiment,  $\blacktriangle$  the 2<sup>nd</sup>,  $\blacksquare$  the 3<sup>rd</sup>, and  $\blacklozenge$  is a 4<sup>th</sup> experiment. Right: A trendline is inserted to provide information on slope and intercept. The line indicating the plateau is calculated as the average of the five points comprising the plateau.

There was an acceptable reproducibility, although the solubility from the first experiment tends to be slightly higher when compared to experiments two and three – the fourth



experiment did not contain CD concentrations in the lower area. The trendline seen on the right side of the figure is therefore calculated on the basis of all four experiments and has the equation  $y = 2.1369x + 0.0204$  giving a  $G_0$  of 20.4 mM. This is highly consistent with the measured  $G_0$  of 20.5 mM but far from the literature data of 32.8  $\mu\text{M}$  (Wishart *et al.*, 2008). A slope larger than 1 indicates a stoichiometry of higher order with respect to the guest but calculating the stoichiometry from the diagram according to the theory (see section 2.1) gives the result 1.1:1 which must be interpreted as a simple 1:1 complex. A slope of approx. 2 means that for each mole of CD, 2 moles of FLU is solubilised. Still, the calculations are based on the plateau, which is the one point of the diagram where the exact amount of CD on complexed form is known as well as the amount of compound on complexed form. However, the plateau is formed at relatively high CD concentrations and this might be a problem. High concentrations are prone to create situations deviating from ideality, which means, that simple assumptions are far from being sufficient in order to describe the situation, for instance, the use of concentrations in calculations is no longer correct and activities must be used instead. On the other hand, the linear part of the diagram is formed in a more diluted environment which should be closer to the theory. Moreover, the plateau was not reproduced, whereas the linear part was comprised by three different experiments. The only option left to determine the stoichiometry is therefore to calculate the stability constant using different values of  $m$ . To obtain a positive stability constant by the use of equation (6) the stoichiometry must be at least a 1:3, i.e.  $m=3$ ; this leads to a stability constant of  $291,338 \text{ M}^{-3}$ . Using equation (7) with  $m=2$  yields a stability constant of  $1067 \text{ M}^{-2}$ . With a 1:1 stoichiometry equation (7) yields a constant of  $78.4 \text{ M}^{-1}$ . As FLU is a small molecule the spatial fit into the  $\gamma$ -CD may be less optimal, meaning that the van der Waal forces driving the complexation become weak, hence, producing the low stability constant. Furthermore, as mentioned in section 2, a small fraction of the FLU molecules has a charge at pH 6.5. Liu & Guo (2002) has shown that ion-dipole interactions do not improve complexation, on the contrary, the interaction between water and the ion seems more favourable. This would explain the low stability constant of a 1:1 complex. However, the results of Ueda & Perrin (1986) are in direct contrast to this. Using microcalorimetry, a stability constant of  $3054 \text{ M}^{-1}$  was calculated for a 1:1  $\gamma$ -CD-FLU complex at pH 7; FLU was considered fully deprotonised. It was claimed to be an order of magnitude higher than a stability constant determined for completely protonised FLU,

although these results were not shown, and the conclusion was that the carboxylate group was important for complex formation.

#### 4.1.5 The complex between ibuprofen and $\gamma$ -cyclodextrin

The CD-IBU diagram, figure 13, is comprised of three identical experiments performed individually, marked with purple, green, and blue on figure to the left.

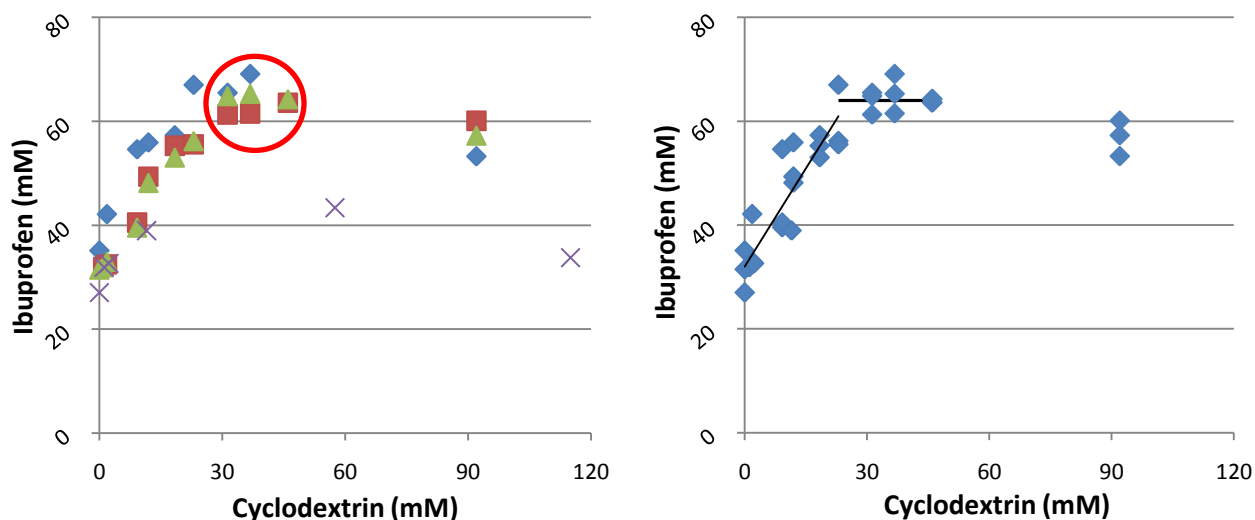
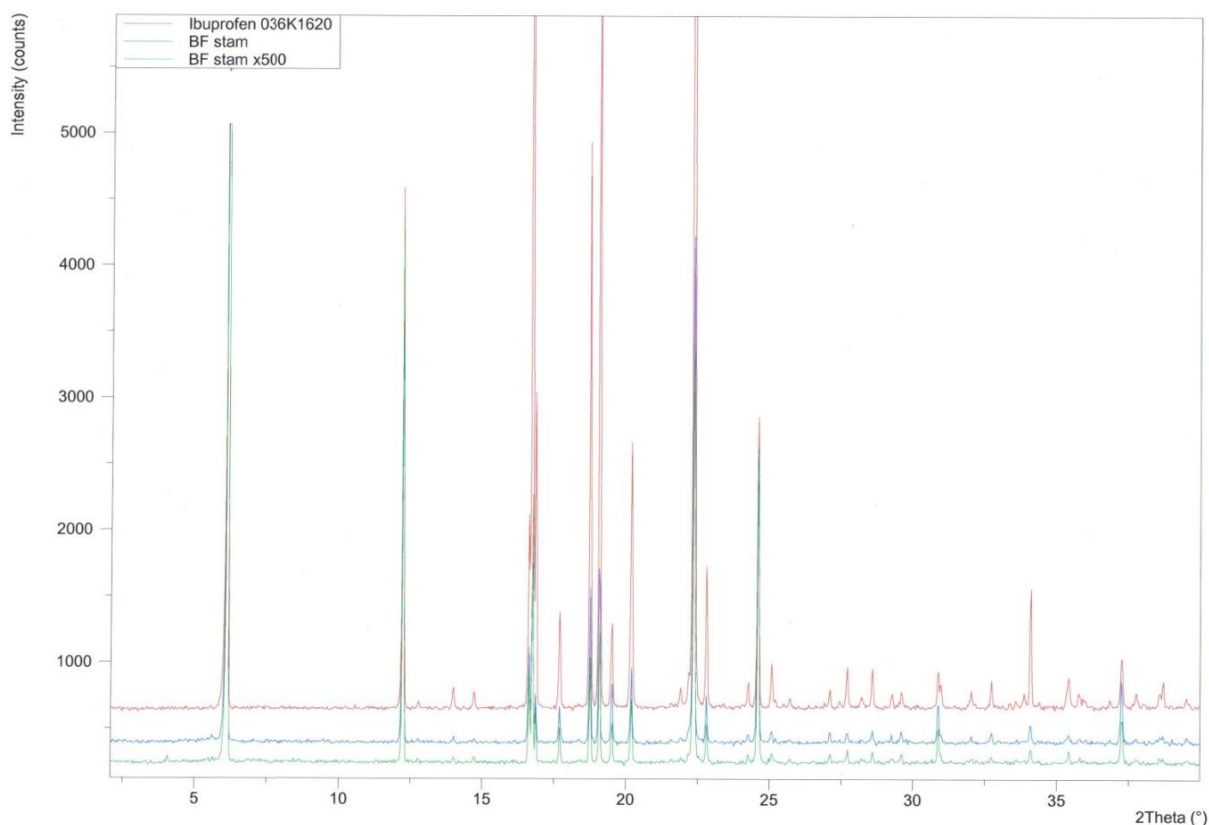


Figure 13: Higuchi-Connors diagram of the complex between ibuprofen and  $\gamma$ -cyclodextrin. Left: The graph is comprised of three identical but independent experiments as well as a plot of the result of a yet another filtration after a standstill of 12 hours:  $\times$  is the 1<sup>st</sup> experiment,  $\blacktriangle$  the 2<sup>nd</sup>,  $\blacksquare$  the second filtration of the samples from the 2<sup>nd</sup> experiment after a 12 hour period, and  $\blacklozenge$  is a 3<sup>rd</sup> experiment. Right: A trendline is inserted to provide information on slope and intercept.

The day after HPLC analysis of the second experiment precipitations were observed in the vials. The precipitate was not resolubilised even after sonication and tumbling at 37 °C. Consequently, the samples were refiltrated and reanalysed and the result is depicted as the red squares. As a result of the experience, the samples of the 3<sup>rd</sup> experiment were filtrated twice with a 12 hours interval before being analysed. As usual, the right side graph shows the trendline of the linear part as well as an indication of the plateau. Creating the CD-IBU diagram was without any doubt the most difficult of them all. Two experiments were discarded as the data could not be internally validated and the remaining four experiments are dubious to say the least. The refiltration of the samples of the second experiment does not seem to have removed any compound, if anything, there seems to be slightly more IBU solubilised. A kind of supersaturation takes place, which further is supported by the observed precipitation. It is quite unclear, though, what should have initiated this supersaturation. The pH adjustment was carried out with 2 M NaOH. Although only a few  $\mu$ l were added at the time, it may have been enough to cause a local rise in temperature thus prompting a “local”

supersaturation. Even if this were the case, it seems unlikely that such a local supersaturation would not precipitate as soon as the vial was replaced in the tumbler returning the solution to normal. On the other hand, even after a new sonication and 3 days in the tumbler at 37 °C the precipitate could not be resolubilised. The only difference between the onset of the experiment and these three days is the pH adjustment, indicating that the pH adjustment must be related to the supersaturation. Following these considerations, a sample of IBU precipitate was investigated by XRPD as described in section 3.2, but as seen on the diffractogram, figure 14, no structural alterations can be detected. This holds true both for a sample with both high (meaning more of the compound is complexed and consequently larger pH fluctuations) and low CD concentrations. This means that salt formation cannot explain the solubility phenomenon.



**Figure 14:** The diffractogram of the x-ray analysis of pure ibuprofen (top) and a precipitate of two vials with high (middle) and low (bottom) CD concentration. The baselines have been graphically moved in order to ease the comparison.

IBU was the only compound, where a precipitation was observed and the compound with the lowest reproducibility. FLU had similar tendencies although not to the same extent. This would make sense since IBU and FLU resemble each other with similar  $pK_a$  values. The two outliers of experiment 1 is another curious problem. They could be a reflection of the supposedly supersaturation problem, however, these two data points differ so significantly

from the rest that it is more likely to be the same problem as with the outlier of the CD-BEN diagram (figure 9): either lack of compound or sampling/handling error. Since it is not possible to give any plausible reason to reject other data points as plain experimental errors, the trendline is calculated on the basis of every data point apart from the two mentioned from experiment 1, as seen on the figure to the right. This results in a trendline with the equation  $y = 1.262x + 0.032$  giving a  $G_0$  of 32 mM. Not surprisingly, this is far from the literature value of 53  $\mu\text{M}$  (Haynes, 2010). However, as opposed to the CD-BEN diagram the measured  $G_0$  of IBU, with a value of 31.2 mM, is consistent with the rest of the data points and therefore also with the calculated 32 mM and for this reason the value is used in the following calculations. The large deviation between the literature value and  $G_0$  could be yet another indication of a supersaturation. The slope is 1.3 which could well indicate a 1:1 stoichiometry. As with FLU, the slope is larger than 1 meaning a negative stability constant. Due to the lacking knowledge of total amount of added IBU, equation (7) cannot be used directly, however, if it is assumed that the diagram represents the reality, the plateau should equal the total amount of IBU in solution,  $G_t$ . There is quite a gap between the last two data points of the CD concentration, which means that it is unknown where the curve begins its descend. The value of  $H_t$  must therefore be somewhere between the two data points. With this assumption, at least an estimate of the stability constant could be given within an interval. With  $G_t=64$  mM and  $H_t$  equals either 46 or 92 mM the stability constant, assuming 1:1 stoichiometry and ideality, is in the range of 16.7-71.9  $\text{M}^{-1}$ . With the assumptions in mind, this is probable if compared to the stability constant of CD-FLU (78.4  $\text{M}^{-1}$ ) considering the chemical equality of the IBU and FLU. Assuming a 1:2 stoichiometry equation (6) can be used to calculate the stability constant. This results in a stability constant of 1676  $\text{M}^{-2}$ , which is the same magnitude as the CD-FLU 1:2 constant. It is likely that the contemplations regarding the CD-FLU complex are the same for CD-IBU due to their chemical similarity. Woldum *et al.* (2008) reports a stability constant for the  $\gamma$ -CD-IBU complex of 265  $\text{M}^{-1}$  determined with a Higuchi-Connors diagram. The experiment was performed with a pH of 3, meaning a large fraction of IBU was protonated and thus without any charge. Larsen *et al.* (1998) used capillary electrophoresis to determine the stability constant of a complex between  $\gamma$ -CD and the IBU anion to be 67  $\text{M}^{-1}$ . It has not been possible to find any reports on stoichiometries other than 1:1 and for this reason the 1:1 stoichiometry and the relating stability constant are deemed the most probable.

#### 4.1.6 The complex between halofantrine and $\gamma$ -cyclodextrin

The next figure, figure 15, shows the making of a Higuchi-Conners diagram of the CD-HAL complex.

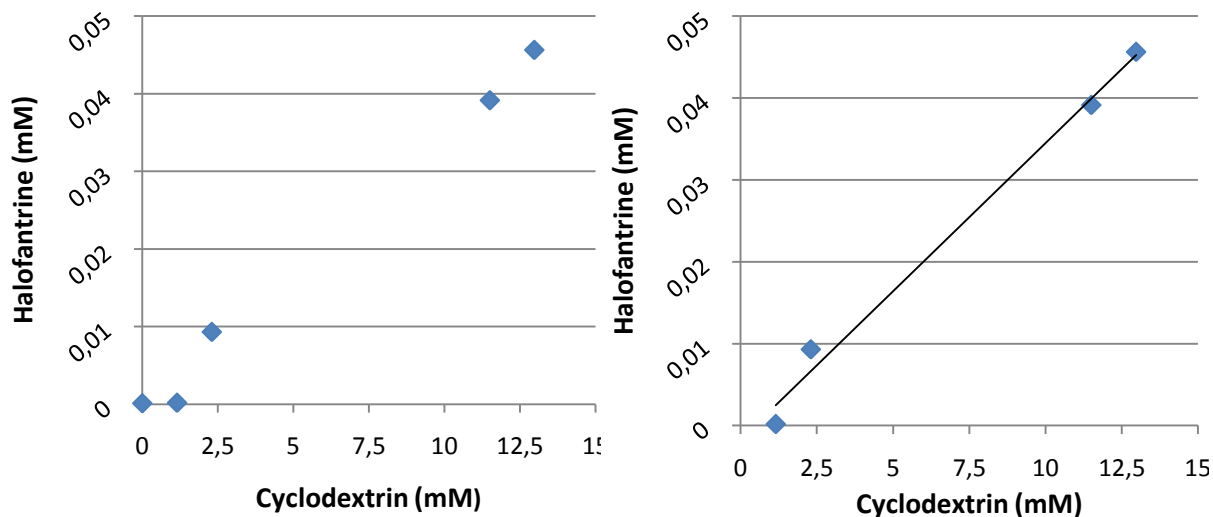


Figure 15: Higuchi-Conners diagram of the complex between halofantrine and  $\gamma$ -cyclodextrin. The graph is comprised of just one experiment shown on the left, while the right shows the insertion of a trendline.

Constructing the Higuchi-Conners diagram for HAL was troublesome. The first three experiments failed miserably with mysterious pH readings, the compound clogging the HPLC column, and data that were not even near anything meaningful. It turned out that the compound was not the free base of halofantrine but most likely some salt, probably an acetate salt. The result of a fourth experiment with a new batch of HAL is shown on the figure, the preceding three can be seen on the data disc. It was meant as a test of the new compound which explains the few data points. A fifth experiment with 10 more points were carried as a continuation of the fourth experiment, that is, with CD concentrations from 12-115 mM. The result of this was a more or less straight line which was reproduced in a sixth experiment. The line is not a plateau, at least not in the sense discussed so far, since the ordinates are in the area of 2  $\mu$ M and well below most of the other data points. It seems as while the added CDs may promote the solubility, “something” is pulling the solubility in the other direction. What this “something” is is unknown but salt formation, which probably caused all the initial challenges, cannot be eliminated until a XRPD analysis can be performed. However, it is peculiar, that this opposite force is exactly the same numerical magnitude as the solubility effect of the CDs no matter the concentration which would seem to be the only explanation to a straight line. A conclusion to what phenomenon caused the straight line was not reached but despite the few data points, a straight line did form from the fourth experiment. With a

determination coefficient of 0.99 and the fact that the data points are situated in the low CD concentration area, it is considered acceptable to look upon the graph as the other diagrams described above and use the data points for the following calculations.

Loftsson *et al.* (2005) constructed a diagram from CIN and HP- $\beta$ -CD which looks quite similar to the CD-HAL diagram with an exponential-like development in the beginning. Had a CD-free sample been made in the CD-CIN experiment it is likely that the same development could have been seen there as well. As described, the phenomenon as thought to be caused by self-association of the compound caused mainly by its lipophilicity. The consequence is, as with CD-CIN, that the interception point with the y-axis is negative. However, a CD-free sample was analysed giving an intrinsic solubility of 115 nM. This is actually not that far from the somewhat imprecise value stated in Kaukonen *et al.* (2004) of <0.1  $\mu$ g/ml corresponding to 200 nM. Inserting a trendline on the linear part of the curve, as does Loftsson *et al.* (2005), the equation  $y = 3.6165 \cdot 10^{-3} x - 1.6718 \cdot 10^{-3}$  is obtained giving a slope of  $3.62 \cdot 10^{-3}$ . Using this and the measured  $G_0$  of 115 nM the stability constant is  $31,650 \text{ M}^{-1}$  assuming 1:1 stoichiometry. It has not been possible to find any reports on  $\gamma$ -CD-HAL complexes in the literature. A 1:1 complex between the HCl salt of HAL and HP- $\beta$ -CD has been reported to have a stability constant of  $2300 \text{ M}^{-1}$  determined with Higuchi-Connors diagrams (Onyeji *et al.*, 2007).

To summarize, the stability constants and stoichiometries are listed in table 2.

**Table 2: The table shows the calculated stability constants of the experiments as well as the used stoichiometries. \*Assumed stoichiometry # Calculated stoichiometry.**

	BEN	CIN	DAN	FLU	IBU	HAL
Stoichiometry	1:1*	1:1*	1:1*	1:1#	1:1*	1:1*
Stability constant ( $\text{M}^{-1}$ )	61,240	2735	6709 50,855	78.4	16.7-71.9	31,650
Literature values ( $\text{M}^{-1}$ )	36,510- 37,940	-	-	3054	67	-

At a first glance, the Higuchi-Connors solubility diagrams are an easy applicable method only provided that a suitable detection method for the compound in question is known. The method is apparently straight-forward if HPLC systems with a ready-to-use setup are available. If, on the other hand, the detection method is unknown or not available it is a relatively hideous process and time-consuming to begin a search of appropriate methods just to be able to analyse the concentration of solubilised product. However, as the above results indicate, determining the stability constant from a Higuchi-Connors solubility diagram has quite a few

major disadvantages. First and foremost, the theory requires ideal solutions, meaning that all particles in the solution, that is complexes, drugs, and CDs, act independently of each other. Second, according to equations (6) and (7), the calculated stability constant is highly dependent of the accuracy of  $G_0$ , the interception of the y-axis. If  $G_0$  does not represent the true intrinsic solubility, the stability constant will be miscalculated. Loftsson *et al.* (2005) have shown that the solubility diagrams provide a good estimate of  $G_0$  if the true intrinsic solubility is above 1 mM. If the solubility is below 0.1 mM,  $G_0$  will most often be much smaller than the true value. All literature values in the present study were far below 0.1 mM, and all the  $G_0$ 's were overestimated. The reason could be a reflection of the necessity of producing results fitted to an ideal solution in order for the theory to be valid. Overall, the fact is that stability constants determined by Higuchi-Connors diagrams are observed stability constants that may, but most likely may not, be equivalent to the true stability constant. Several complexes can be formed, both inclusion and non-inclusion, aggregations can occur, both between cyclodextrins and between drugs, and perhaps supersaturation may occur. It has been shown that aggregation between CDs, stabilised by networks of hydrogen bonds, are concentration dependent, increasing with increasing concentration, which most certainly is a problem when determining stability constants with Higuchi-Connors diagrams. It is an evident problem if the apparent constant determined by the experiments is, in fact, a sum of several constants describing numerous complexes (Loftsson *et al.*, 2007). Most aggregates observed are small, in most cases, that is, below 20 nm and well below the cut-off of the filters. Bigger sizes have been seen, though, with the consequences that they may be filtered out but also that yet another type of complexes can be formed reminiscent of micelles. This has been shown to happen between HP- $\beta$ -CD and IBU which could explain the low reproducibility of the CD-IBU diagram (Brewster & Loftsson, 2007). It could be very interesting to perform NOESY/ROESY NMR on the complexes in order to try and gain a better understanding of the complexation and thereby to understand the behaviour of the solubility profiles better.

An alternative method to stability constant determination could have been chosen or at least used as a means of confirmation of the obtained results. Affinity capillary electrophoresis (ACE), NMR, and isothermal titration calorimetry (ITC) are methods that were readily available to the project. However, the disadvantage of determining stability constants from NMR and ACE is that it requires the use of appropriate software that can perform a non-linear

regression fairly precise and preferably effortlessly. NMR analysis of the large compounds and the cyclodextrin might result in quite complex spectra although the compounds of the present project all include aromatic protons which have a rather distinct, and therefore traceable, shift facilitating the analysis. ACE will result in a much simpler spectrum considering only one peak will be present since CDs do not absorb UV radiation. It is evident that the use of ACE requires that the complexes hold a charge either from the guest or from the host – or both as long as they do not cancel each other. Since CDs are neutral, it means that the technique is not applicable to BEN. Another requirement is that the guest has to be soluble enough in the buffer used in order to be detected which very well could turn out to be a problem when working with compounds that are highly insoluble in aqueous buffers. NMR and ITC offer the possibility of using more organic solvents but that would alter the stability constant and it would not be comparable to stability constants obtained in aqueous buffers. However, as stated in section 2.1, the purpose of the experiments was not to determine an exact value of the stability constant but to find the relative affinity ratio between the six compounds and  $\gamma$ -CD. This means that as long as all complexes are tested with the same method the relative stability constants should be comparable. The stability constants obtained in the present work may not be the true values of the complexes and the proportional difference between the complexes may not be correct – for instance, the magnitude of the stability constant of the CD-BEN complex may not be 10 times as high as that of CD-DAN as indicated, but in reality only 4 times – but proportionally the stability constants found in this project are deemed to be acceptable. It seems likely that HAL and BEN, logD of 5.6 (pH 7) and 6.2, respectively, have the highest stability constants and IBU and FLU, logD of  $\sim$ 2 and  $\sim$ 0.9 (pH 7.4), respectively, the lowest when considered their hydrophobicity, as reflected by their logDs.

## **4.2 The degradation of cyclodextrins by various $\alpha$ -amylases**

The degradation reactions were carried out at 37 °C and in a TRIS-maleate buffer with an ionic strength of 150 mM and pH 6.5 in order to mimic the environment of the small intestine. 4 mM CaCl<sub>2</sub> was added to secure the function of the enzyme. Substrate concentration in all experiments was 5 mM, and enzyme concentration was approx. 55 units/ml. The progress of the reaction was followed by measuring the amount of reducing ends as maltose equivalents. The degradation products are all reducing sugars which means that when added to a 3,5-



dinitrosalicyl acid solution the latter is reduced to 3-amino-5-nitrosalicylic acid which absorbs strongly at 540 nm. The absorbance results are then compared to a maltose standard curve.

#### 4.2.1 Porcine pancreatic $\alpha$ -amylase

The degradation of all native CDs as well as the hydroxypropyl derivatives of  $\beta$ - and  $\gamma$ -CD by porcine pancreatic  $\alpha$ -amylase was investigated and the results are shown in figure 16 below.

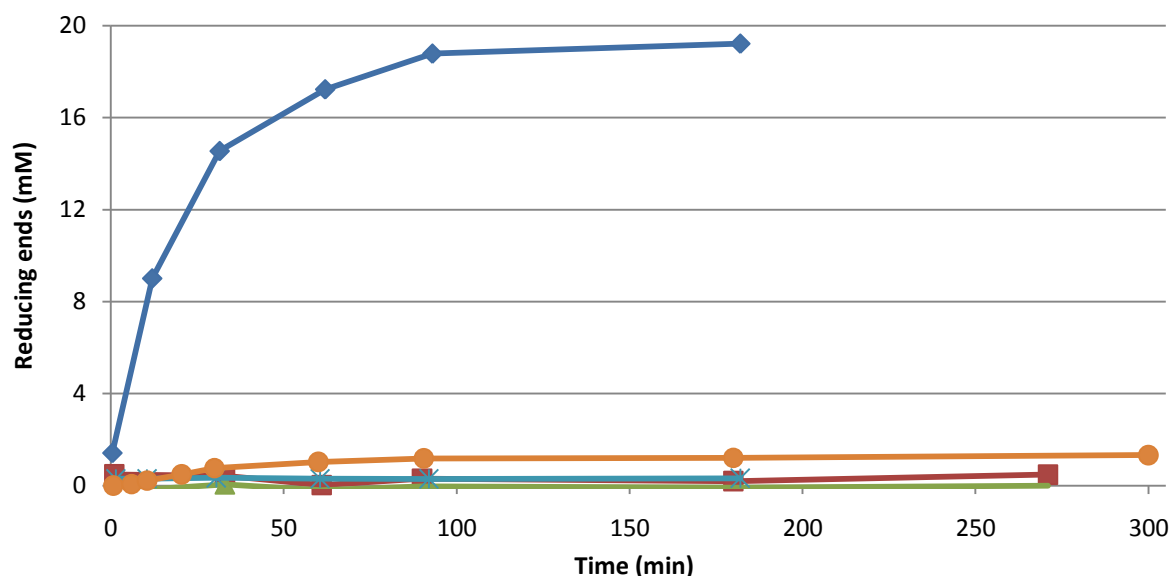


Figure 16: The figure shows the degradation of 5 mM native cyclodextrins and the hydroxypropyl derivatives of  $\beta$ -CD and  $\gamma$ -CD by porcine pancreatic  $\alpha$ -amylase. —  $\alpha$ -cyclodextrin; —  $\beta$ -cyclodextrin; —  $\gamma$ -cyclodextrin; — HP- $\beta$ -cyclodextrin; — HP- $\gamma$ -cyclodextrin.

Not surprisingly, compared to earlier results,  $\gamma$ -CD is almost fully reduced by the amylase. In the experiment conducted by Kondo *et al.* (1990) only 80% of the  $\gamma$ -CD was degraded after 24 hours but it should be noticed that the enzyme concentration used was 50 nm whereas the concentration in the present experiment was approx. 38  $\mu$ M (the exact molecular mass of the enzyme is unknown but according to the manufacturer somewhere between 51-54 kDa). The amount of undigested CD remaining in the solution was not measured but, assuming that the degradation product is maltose, a full degradation should result in 20 mM reducing ends which means that 96 % of the  $\gamma$ -CD is converted to maltose (the amount of reducing ends formed after three hours were 19.22 mM). However, according to Robyt and French (1970) a relatively substantial amount of glucose is also formed, which means that the total amount of reducing ends is somewhat higher than 20 mM rendering the 96 % a mere estimate. It should also be noted that it seems as if no  $\text{Ca}^{2+}$  was added in the experiment by Kondo *et al.* (1990) which can further explain the relatively big difference in amount of degraded CD.

As seen on the figure,  $\alpha$ - and  $\beta$ -CD are not degraded. Marshall & Miwa (1981) showed that with an enzyme concentration of 8.7  $\mu$ M 20% of  $\beta$ -CD would be degraded after 24 hours. It was not possible to reproduce these results even though four times as much enzyme was used. However, generally with all enzymes used it was observed that incubation longer than 12 hours resulted in depletion of the observed amount of reducing ends. Sterile vials and buffers were used but due to sampling the vials were opened frequently in a none-sterile environment. The reaction conditions are optimal growths conditions to many bacteria and the observed depletion in the amount of reducing ends is most likely caused by bacteria digesting the sugars. In future experiments the problem can be solved by adding antibacterial compounds, i.e. sodium azide, which will not form complexes with the CDs, inhibit the enzyme, or in any other way interfere with the reaction.

It was a surprise to find that HP- $\gamma$ -CD is partially degraded. The batch was analysed on a mass spectrometer and proved to be free of native  $\gamma$ -CD, the chromatogram can be seen in appendix II. The substitution degree was not determined but the degradation is assumed to be much dependent on the degree of substitution: the more substituted the lesser degraded.

The Michaelis-Menten constants of the hydrolysis of both  $\gamma$ -CD and HP- $\gamma$ -CD were determined by non-linear regression of the saturation curve using SigmaPlot (Systat Software, Inc., v. 11.0). The plot of  $\gamma$ -CD is shown on figure 17, while the plot of HP- $\gamma$ -CD is shown on figure figure 18.

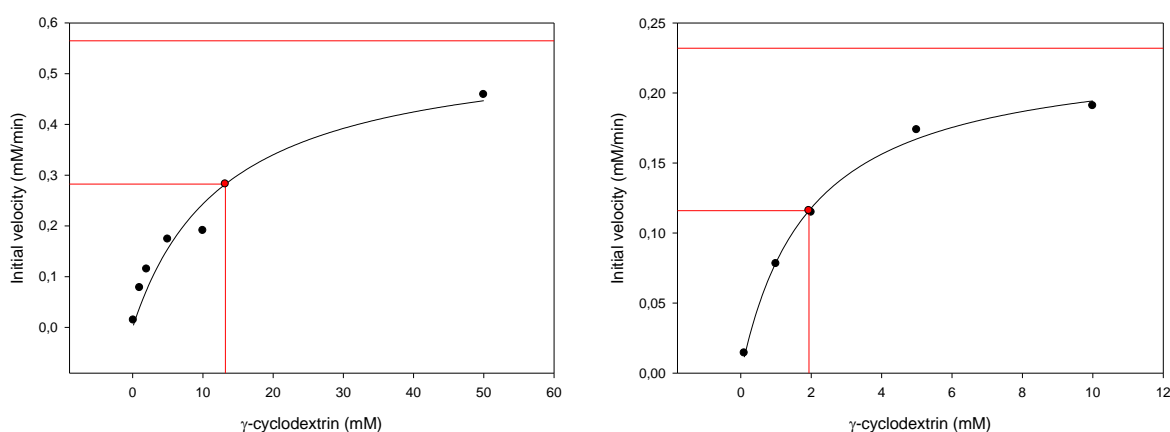


**Figure 17: The saturation curve of the enzymatic degradation of  $\gamma$ -cyclodextrin porcine pancreatic  $\alpha$ -amylase. The horizontal line in the top represents  $V_{max}$  and the red data point is artificially inserted and indicates  $K_M$ . The graph on the left is the plot including the x-value 50 mM while the graph on the right is excluding this value.**

The horizontal red line is representing  $V_{max}$  while the red data point on the curve is manually inserted and is representing the  $K_M$ -value. As seen on the figure two very different results can

be obtained depending on which data point is seen upon as the outlier. The figure to the left shows the result when all data points is used. The substrate concentration of 10 mM is seen as an outlier and non-linear regression yields the values 0.5648 mM/min and 13.2072 mM for  $V_{\max}$  and  $K_M$ , respectively, and a coefficient of determination of 0.946. This is a very high  $K_M$  indeed compared to the Marshall & Miwa result of 0.97 mM, see table 1. If, however, substrate concentration 50 mM is seen as the outlier, the result is a  $V_{\max}$  of 0.2320 mM/min and a  $K_M$  of 1.9373 mM with the coefficient of determination of 0.997. The initial velocity is determined as the slope of the initial rate period, that is, the linear part of the degradation curve. The curve of substrate concentration 50 mM was poor with a determination coefficient of only 0.84 and it is therefore likely that something has gone wrong during the experiment resulting in an incorrect slope and thereby in an incorrect data point in the saturation curve. For this reason, it is considered best to exclude the data point, thus rendering the Michaelis-Menten constants of 0.2320 and 1.9373 to be more correct.

The Michaelis-Menten plot of the degradation reaction of HP- $\gamma$ -CD is, as mentioned, shown on figure 18.

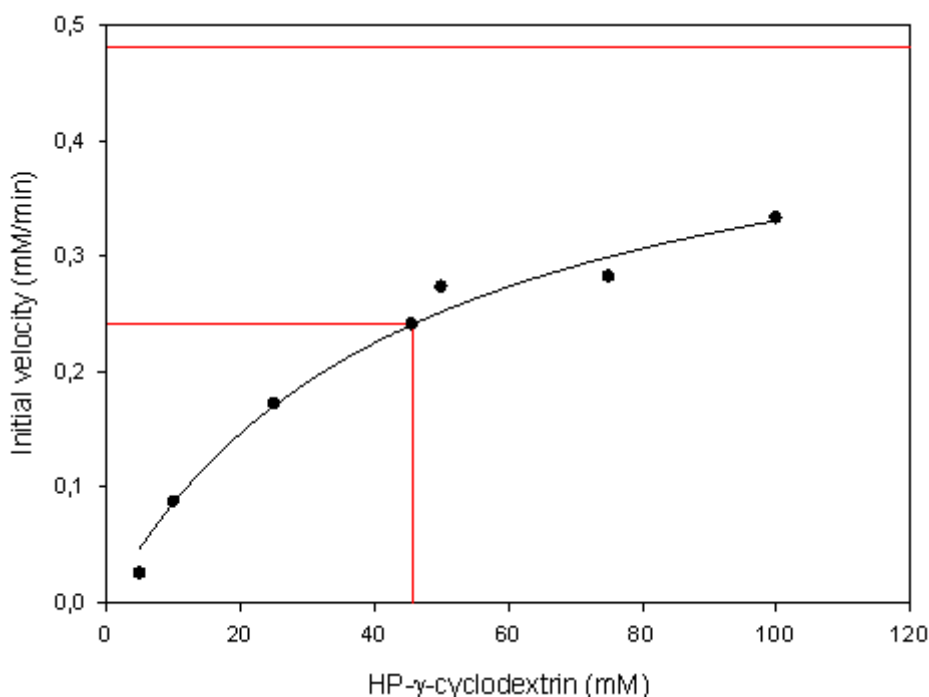


**Figure 18:** The saturation curve of the enzymatic degradation of HP- $\gamma$ -cyclodextrin using porcine pancreatic  $\alpha$ -amylase. The horizontal line in the top represents  $V_{\max}$  and the red data point is artificially inserted and indicates  $K_M$ .

As with the curve of  $\gamma$ -CD the red horizontal red line indicates  $V_{\max}$  whereas the red data point is manually inserted in order to indicate  $K_M$ . Non-linear regression yields a  $K_M$  of 45.637 mM

and a  $V_{\max}$  value of 0.4818 mM/min. The degradation of HP- $\gamma$ -CD has seemingly not been reported before and it has therefore not been possible to find any literature values to use in a comparison. The  $K_M$  value is high indicating low affinity for the enzyme-substrate complex. This is expected since the hydroxypropyl-group must cause some steric hindrance, perhaps amongst other things, at the active site which impedes the access to the site and thereby the affinity and degradation.

#### 4.2.2 Human pancreatic and salivary $\alpha$ -amylase

Neither of the human enzymes hydrolyses  $\alpha$ - and  $\beta$ -CD, as seen on figure 19, which is the same result as obtained by Kondo *et al.* (1990), while Marshall & Miwa (1981) reports a hydrolysis of  $\beta$ -CD as “extremely slow” without elaborating further on the matter. The degradation of the hydroxypropyl derivatives were not investigated.

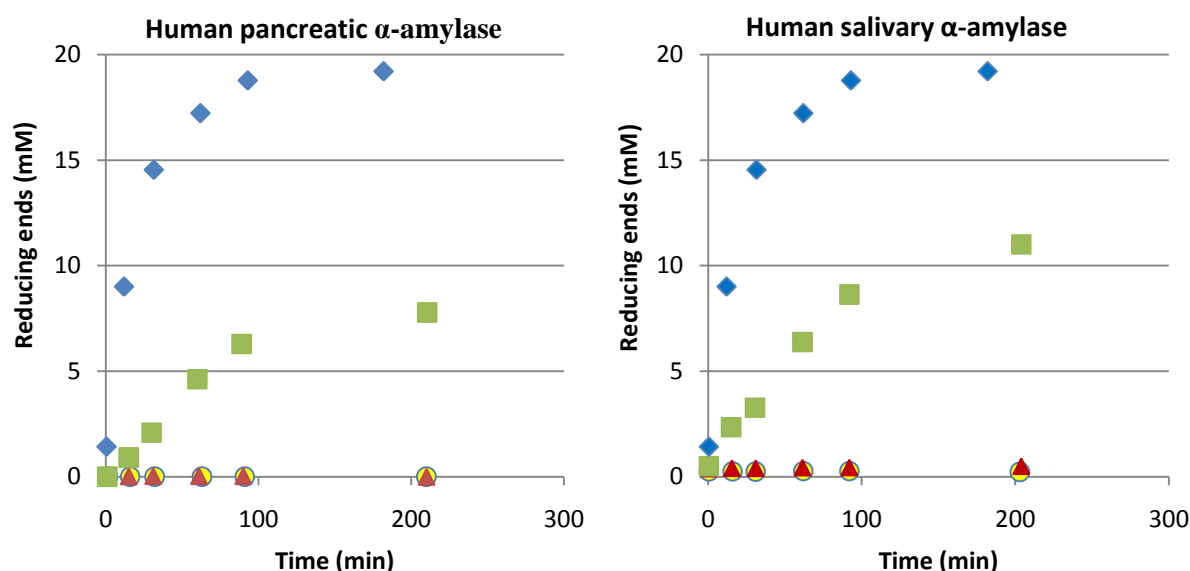


Figure 19: The figure shows the degradation of 5 mM native cyclodextrins by human pancreatic  $\alpha$ -amylase on the left and human salivary  $\alpha$ -amylase on the right.  $\bullet$   $\alpha$ -cyclodextrin;  $\blacktriangle$   $\beta$ -cyclodextrin;  $\blacksquare$   $\gamma$ -cyclodextrin;  $\blacklozenge$   $\gamma$ -cyclodextrin degraded by porcine  $\alpha$ -amylase, see figure 16.

Both enzymes hydrolyse  $\gamma$ -CD although human salivary  $\alpha$ -amylase is somewhat faster than the pancreatic counterpart. This is in contrast to the findings of Marshall and Miwa (1981) that are the exact opposite. The Michaelis-Menten constants for the two human enzymes were not determined, which is an obvious experiment in the near future, but it would have been interesting to compare the constants obtained from the present experiment with those of Marshall & Miwa. An estimate of the differences between the two experiments can be seen when comparing mid-way results. Marshall & Miwa states that after 30 minutes 9  $\mu$ g/0.5 ml and 29.8  $\mu$ g/0.5 ml glucose is formed in the reaction with salivary and pancreatic amylase,

respectively. This is equivalent to 100  $\mu\text{M}$  and 331  $\mu\text{M}$ . In comparison, 3.3 mM and 2.1 mM reducing ends were formed in the present reactions with salivary and pancreatic amylases, respectively. Of course, the results cannot be compared directly due to differences in enzyme concentration and reaction products measurement but it is noteworthy to see that in the Marshall & Miwa experiment the pancreatic enzyme is three times as fast as the salivary enzyme whereas in the present experiment the salivary enzyme is 1½ time as fast than the pancreatic enzyme. Both enzymes in both experiments were added so that their individual activity towards starch was the same so no apparent explanation to the differences is available.

### 4.2.3 Comparison between the porcine and human amylases

Porcine amylase degrades  $\gamma$ -CD faster than both human enzymes - figure 20 shows the direct comparison between the hydrolysis of  $\gamma$ -CD by the three amylases.

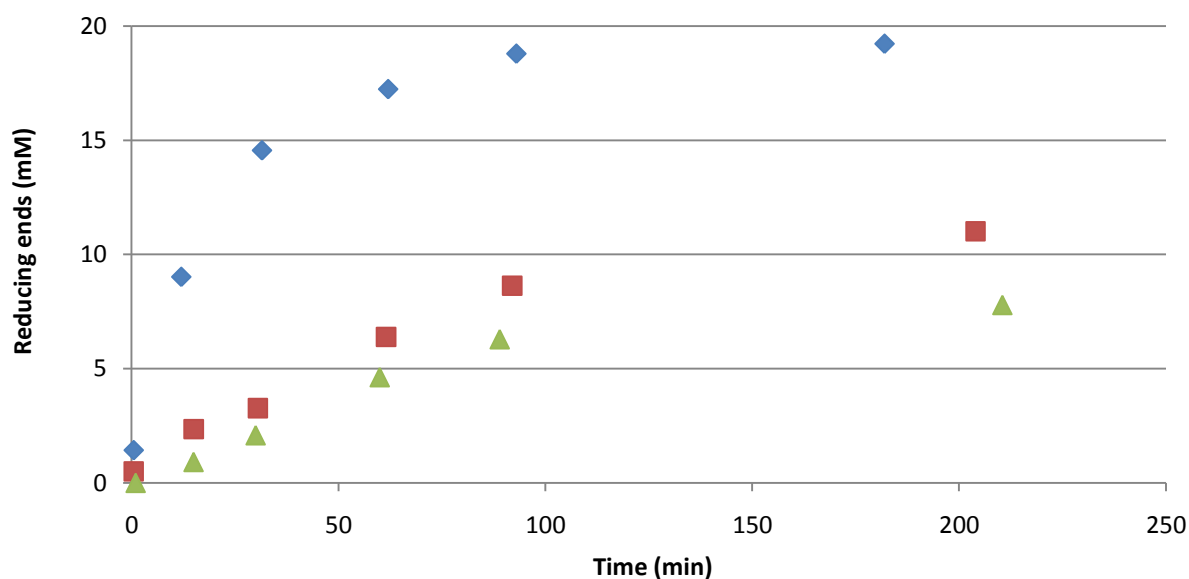


Figure 20: The figure shows the hydrolysis of 5 mM  $\gamma$ -cyclodextrin by porcine pancreatic  $\alpha$ -amylase ( $\blacklozenge$ ), human salivary  $\alpha$ -amylase ( $\blacksquare$ ), and human pancreatic  $\alpha$ -amylase ( $\blacktriangle$ ).

The slopes in the initial rate period of the three reactions are determined as 0.079, 0.093, and 0.408 mM/min for human pancreatic, human salivary, and porcine pancreatic enzyme, respectively, giving an indication of the different enzyme efficiencies. Robyt & French (1967) compared the action patterns of  $\alpha$ -amylases from porcine pancreas, human saliva, and *A. oryzae* of the hydrolysis of amylose. The degree of multiple attack of porcine amylase was found to be three times as high as that of the human amylase. Due to the different substrates used the results cannot, of course, be directly compared but it must be assumable that the

porcine amylase is more efficient than its human and bacterial counterparts which is consistent with the present results.

As seen on figure 20 the first data points are not situated at the origin as could be expected. First of all, this is caused by the fact that the set-up made it impossible to sample immediately after enzyme addition – the reaction was not stopped before 30-60 seconds after enzyme addition. Second, although the eppendorf tubes used to heat the samples for analysis were preheated to approx. 95 °C, the formation of a heat gradient cannot be eliminated meaning that it is possible that further seconds passed before the reaction was, in fact, stopped.

#### 4.2.4 Degradation of $\gamma$ -cyclodextrin in the presence of $\alpha$ -cyclodextrin

As mentioned in chapter 1, Kondo *et al.* (1990) showed that *in vitro*, when the main substrates of the enzymes are present in the reaction media, the native CDs function as competitive inhibitors of the hydrolysis. It was not shown, however, what impact on the reaction the CDs have on each other. Since it has been shown both in earlier and in the present experiments that  $\alpha$ -CD is not degraded by any amylase, the porcine amylase was added to a solution of various molar ratios of  $\gamma$ - and  $\alpha$ -CD and the result is shown in figure 21.

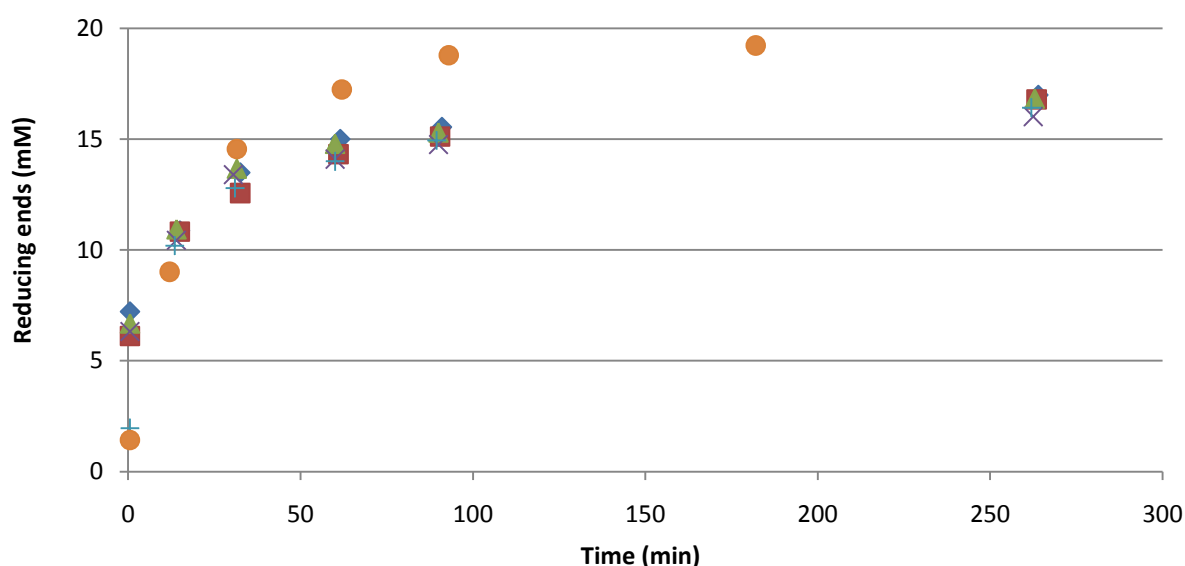


Figure 21: The degradation of 5mM  $\gamma$ -CD in the presence of  $\alpha$ -CD at various molar ratios by porcine  $\alpha$ -amylase.  $\blacklozenge$   $\gamma$ -CD: $\alpha$ -CD 5:1;  $\blacksquare$   $\gamma$ -CD: $\alpha$ -CD 5:2;  $\blacktriangle$   $\gamma$ -CD: $\alpha$ -CD 5:3;  $\times$   $\gamma$ -CD: $\alpha$ -CD 5:4;  $+$   $\gamma$ -CD: $\alpha$ -CD 5:5;  $\bullet$  5 mM  $\gamma$ -CD from figure 16.

No obvious connection between the molar ratios can be established but it is clear that  $\alpha$ -CD exhibits some inhibitory effect on the degradation. It would be very interesting to look into the matter further not only by determining and comparing Michaelis-Menten constants but

also by, for instance, investigating the quantity needed to completely inhibit the reaction, if possible.

### 4.3 The degradation of cyclodextrin inclusion complexes by porcine $\alpha$ -amylase

The hypothesis in the present thesis was that if cyclodextrin complexes are degraded by the  $\alpha$ -amylases of the small intestine a decrease in bioavailability, as observed with  $\beta$ -CD (Westerberg & Wiklund, 2005), would not occur. Experiments were therefore conducted in order to investigate whether or not the complexes are degraded.

On the figure below, figure 22, is the degradation of the two chosen complexes,  $\gamma$ -CD-FLU and  $\gamma$ -CD-BEN shown.

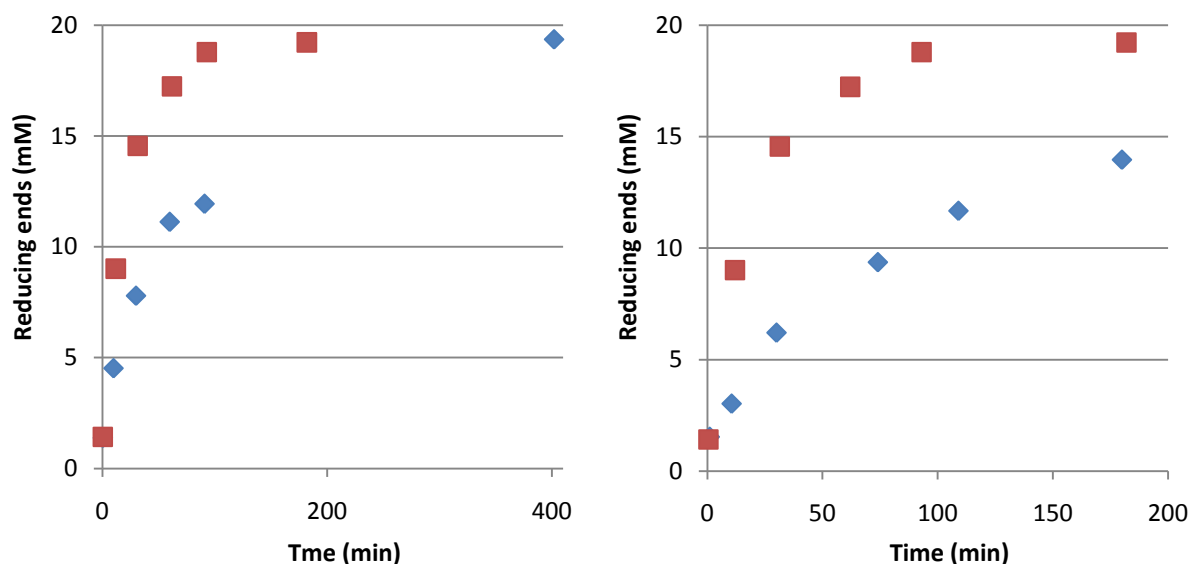


Figure 22: The figure shows the degradation of the  $\gamma$ -CD-FLU complex (left) and  $\gamma$ -CD-BEN complex (right) by porcine  $\alpha$ -amylase.  $\blacklozenge$  complex  $\blacksquare$  5 mM  $\gamma$ -CD from figure 16.

As the figure shows, the complexes are degraded albeit at different rates. It is strange, though, that only  $\sim 14$  mM reducing ends are released from the  $\gamma$ -CD-BEN degradation. As seen on figure 9 less than 0.05 mM BEN is solubilised at a concentration of 5 mM  $\gamma$ -CD. Hence, with a stoichiometry of 1:1 more than 4.95 mM  $\gamma$ -CD should be on the free form; a situation equivalent to that of figure 16 (also depicted in red on figure 22). The  $\gamma$ -CD degradation curve was reproduced several times on different occasions (data not shown), which means that somehow the addition of BEN and/or the formation of a CD-BEN complex has an inhibiting effect on the degradation. It is possible that BEN acts as an inhibitor of the enzyme. It is

considered unlikely, since BEN shows no similarities with the common substrates of amylase. The active site of  $\alpha$ -amylase consists of two residues, Glu and Asp (in their basic forms), that are directly involved in the enzymatic reaction by acting as an acid/base catalyst and a nucleophile, respectively. A second Asp, also in its basic form, is considered part of the active site but function in a more indirect manner as a destabilizer of the substrate by hydrogen bonding to OH2 and OH3 of a glucose unit (van der Maarel *et al.*, 2002). Being apolar it is difficult to see how BEN should interact with the active site. The theory can be verified quite simply by examining the activity of the enzyme before and after BEN addition. However, if the result of such an examination is that BEN is not an inhibitor, another explanation must be found. It can be speculated that the kinetics of the equilibrium between BEN and  $\gamma$ -CD is much faster than between  $\gamma$ -CD and the enzyme. It is assumed that the complex cannot be degraded by the enzyme. The hypothesis would then be that, due to the possible faster  $\gamma$ -CD-BEN equilibrium, the active site of the enzyme cannot interact with the  $\gamma$ -CD before a new complex has formed. This situation could slow the degradation process and create the curve observed on figure 22. Proving the hypothesis is complicated. If it was shown that BEN is not an inhibitor and if it could be verified that the complex is, in fact, not degraded by the enzyme, the answer must lie elsewhere leaving the mentioned hypothesis as a possible solution.

The initial velocities of the complexes were found to be 0.208 mM/min and 0.161 mM/min for  $\gamma$ -CD-FLU and  $\gamma$ -CD-BEN, respectively, which is slower than the native  $\gamma$ -CD. The complex with the high stability constant is therefore degraded more slowly than the complex with the low stability constant. This seems logic as the amylase most likely cannot degrade the complex itself but only the free cyclodextrin which is in equilibrium with the complex. A complex with a high stability constant will be shifted more towards the bound form compared to a complex with a low stability constant. However, in the flurbiprofen experiment the reaction was allowed to continue for 24 hours (see data disc) which resulted in 19.98 mM reducing ends, that is, the  $\gamma$ -CD is nearly fully degraded. However, the retention time in the small intestine is approx. five hours (Martini, 2004) but the amylase concentration is assumed to be higher than 56 units/ml so it is thus considered likely that the free CDs will, in fact, be degraded, regardless of the complex state. This means that the amount of the free CDs will be reduced which, according to Le Chateliers principle, means that the equilibrium will be shifted away from the complex state. As a consequence, it is considered likely that the



situation described by Westerberg & Wiklund (2005) will not occur when using  $\gamma$ -CDs and perhaps even not with HP- $\gamma$ -CDs. Naturally, this hypothesis will have to be confirmed *in vivo*. As pointed out by Westerberg & Wiklund *in vitro* observations can deviate from *in vivo* observations for which reason absolute conclusions should be made cautiously. Obvious future experiments also include the construction of a complete overview of the degradation of  $\gamma$ -CD and HP- $\gamma$ -CD by the pancreatic  $\alpha$ -amylase of often used animal models, i.e. rat, mice, and dog, using the same experimental set-up. In this way, comparable Michaelis-Menten constants can be obtained and possible conclusions can be made as to whether  $\gamma$ -CD and HP- $\gamma$ -CD can be used in the early stages of animal experiments without retarding the absorption of the drug. Questions still remain to be answered regarding complex chemistry and solubility behaviour and a possible future systematic investigation of the degradation of CD complexes should include a thorough characterization of the complexes, i.e. examining orientation, binding sites, and stoichiometry by NMR and study particle size and thus aggregate formation, for instance by dynamic light scattering.

## 5 Conclusion

The purpose of this master's thesis was to investigate the possible influences of complex formation on  $\gamma$ -cyclodextrin ( $\gamma$ -CD) degradation by  $\alpha$ -amylase. It was confirmed that  $\gamma$ -CD is degraded, as the only native CD, by human and porcine pancreatic  $\alpha$ -amylase as well as human salivary  $\alpha$ -amylase. The porcine  $\alpha$ -amylase was found to be the most efficient of the three, with the human salivary  $\alpha$ -amylase being 1.5 times faster than human pancreatic  $\alpha$ -amylase. Hydroxypropyl- $\gamma$ -CD was found to be degraded by porcine pancreatic  $\alpha$ -amylase.  $\alpha$ -CD was shown to have an inhibiting effect on  $\gamma$ -CD degradation although no consistency between inhibiting effect and  $\alpha$ -CD concentration could be established at the concentrations examined.

Stability constants of complexes between  $\gamma$ -CD and ibuprofen, flurbiprofen, danazol, cinnarizine, halofantrine, and benzo[*a*]pyrene was determined using Higuchi-Connors diagrams and the degradation of  $\gamma$ -CD in the presence of flurbiprofen ( $K_{1:1}$ : 78.4) and benzo[*a*]pyrene ( $K_{1:1}$ : 61,240) was investigated. The degradation was found to be partly inhibited by the presence of the complex with the stronger complex being degraded more slowly than the weaker complex. Hence, the conclusion is that complex formation does have an influence on the degradation of  $\gamma$ -CD by slowing the degradation. However, the fact that  $\gamma$ -CD is degraded in spite of the complex indicates that a situation, as described by Westerberg & Wiklund (2005), will not occur when using  $\gamma$ -CD and that  $\gamma$ -CD, could, in fact, be a more suitable vehicle for early animal experiments with new drug candidates. The hypothesis will have to be confirmed *in vivo*.

## 6 References

- ABDULLAH, M., FRENCH, D. & ROBYT, J. F.** 1966. Multiple Attack by  $\alpha$ -Amylases. *Arch. Biochem. Biophys.*, 114, pp.595-598.
- ARTISS, J. D., BROGAN, K., BRUCAL, M., MOGHADDAM, M. & JEN, K.-L. C.** 2006. The effects of a new soluble dietary fiber on weight gain and selected blood parameters in rats. *Metabolism*, 55, pp.195-202.
- BLYSHAK, L. A., DODSON, K. Y., PATONAY, G. & WARNER, I. M.** 1989. Determination of Cyclodextrin Formation Constants Using Dynamic Coupled-Column Liquid Chromatography. *Anal. Chem.*, 61, pp.955-960.
- BREWSTER, M. E. & LOFTSSON, T.** 2007. Cyclodextrins as pharmaceutical solubilizers. *Adv. Drug Deliver. Rev.*, 59, pp.645-666.
- BROWN, N. D., BUTLER, D. L. & CHIANG, P. K.** 1993. Stabilization of thymopentin and preservation of its pharmacological properties by 2-hydroxypropyl- $\beta$ -cyclodextrin. *J. Pharm. Pharmacol.*, 45, pp.666-667.
- BUCKLEY, J. D., THORP, A. A., MURPHY, K. J. & HOWE, P. R.** 2006. Dose-dependent inhibition of the post-prandial glycaemic response to a standard carbohydrate meal following incorporation of alpha-cyclodextrin. *Ann. Nutr. Metab.*, 50, pp.108-114.
- CONNORS, K. A.** 1996. Measurement of Cyclodextrin Complex Stability Constants. In: J. Szejtli and T. Osa, (eds). *Comprehensive Supramolecular Chemistry Vol. 3*, Oxford, UK: Elsevier Science Ltd, pp.205-242.
- FAGERBERG, J. H., TSINMAN, O., SUN, N., TSINMAN, K., AVDEEF, A. & BERGSTRÖM, C. A. S.** 2010. Dissolution Rate and Apparent Solubility of Poorly Soluble Drugs in Biorelevant Dissolution Media. *Mol. Pharm.*, 7, pp.1419-1430.
- FIELDING, L.** 2000. Determination of Association Constants ( $K_a$ ) from Solution NMR Data. *Tetrahedron*, 56, pp.6151-6170.
- HADGRAFT, J. & VALENTA, C.** 2000. pH,  $pK_a$  and dermal delivery. *Int. J. Pharm.*, 200, pp.243-247.
- HARATA, K.** 2006. Crystallographic Study of Cyclodextrins and Their Inclusion Complexes. In: H. Dodziuk, (ed). *Cyclodextrins and Their Complexes*, Weinheim: Wiley-VCH, pp.147-191.
- HAYNES, W. M.** 2010. Relevant tables. In: *CRC Handbook of Chemistry and Physics [online]*, 91st ed. (Internet version 2011): CRC Press/Taylor and Francis, Boca Raton, FL, USA.
- HEDGES, A.** 1998. Industrial Applications of Cyclodextrins. *Chem. Rev.*, 98, pp.2035-2044.
- HENRISSAT, B.** 1991. A classification of glycosyl hydrolases based on amino acid sequence similarities. *J. Biochem*, 280, pp.309-316.

- HICKS, K. B., HAINES, R. M., TONG, C. B. S., SAPERS, G. M., EL-ATAWY, Y., IRWIN, P. L. & SEIB, P. A.** 1996. Inhibition of Enzymatic Browning in Fresh Fruit and Vegetable Juices by Soluble and Insoluble Forms of  $\beta$ -Cyclodextrin Alone or in Combination with Phosphates. *J. Agric. Food Chem.*, 44, pp.2591-2594.
- HIGUCHI, T. & CONNORS, K. A.** 1965. Phase-Solubility Techniques. In: C. N. REILLY, (ed). *Adv Anal Chem Instrum*, vol. 4, New York: Interscience Publishers, pp.117-213.
- HOLM, R., HARTVIG, R. A., NICOLAJSEN, H. V., WESTH, P. & ØSTERGAARD, J.** 2008. Characterization of the complexation tauro- and glycoconjugated bile salts with  $\gamma$ -cyclodextrin and 2-hydroxypropyl- $\gamma$ -cyclodextrin using affinity capillary electrophoresis. *J. Incl. Phenom. Macrocycl. Chem.* , 61, pp.161-169.
- ITO, K., KATO, Y., TSUJI, H., NGUYEN, H. T., KUBO, Y. & TSUJI, A.** 2007. Involvement of organic anion transport in transdermal absorption of flurbiprofen. *J. Control Release*, 124, pp.60-68.
- JADHAV, G. S. & VAVIA, P. R.** 2008. Physicochemical, in silico and in vivo evaluation of a danazol-beta-cyclodextrin complex. *Int. J. Pharm.*, 352, pp.5-16.
- JODÁL, I., KANDRA, L., HARANGI, J., NÁNÁSI, P. & SZEJTLI, J.** 1984a. Enzymatic Degradation of Cyclodextrins; Preparation and Application of Their Fragments. *J. Inclusion Phenom.*, 2, pp.877-884.
- JODÁL, I., KANDRA, L., HARANGI, J., NÁNÁSI, P. & SZEJTLI, J.** 1984b. Hydrolysis of Cyclodextrin by *Aspergillus oryzae*  $\alpha$ -Amylase. *Starch/Stärke*, 4, pp.140-143.
- KAUKONEN, A., BOYD, B. J., PORTER, C. J. H. & CHARMAN, W. N.** 2004. Drug Solubilization Behaviour During *in Vitro* Digestion of Simple Triglyceride Lipid Solution Formulations. *Pharm. Res.*, 21, pp.245-253.
- KOBAYASHI, N., SAITO, R., HINO, Y., UENO, A. & OSA, T.** 1982. Chirality of the Two Pyrene Molecules included in  $\beta$ -Cyclodextrin. *B. Chem. Soc. Jpn.*, pp.706-707.
- KONDO, H., NAKATANI, H. & HIROMI, K.** 1990. In vitro action of human and porcine  $\alpha$ -amylases on cyclo-malto-oligosaccharides. *Carbohydr. Res.*, 204, pp.207-213.
- LIPINSKI, C. A.** 2000. Drug-like properties and the causes of poor solubility and poor permeability. *J. Pharmacol. Toxicol.*, 44, pp.235-249.
- LIPINSKI, C. A., LOMBARDO, F., DOMINY, B. W. & FEENEY, P. J.** 1997. Experimental and computational approaches to estimate solubility and permeability in drug discovery and development settings. *Adv. Drug Deliver. Rev.*, 23, pp.3-25.
- LIU, L. & GUO, Q.-X.** 2002. The Driving Forces in the Inclusion Complexation of Cyclodextrins. *J. Incl. Phenom. Macro.* , 42, pp.1-14.

- LI, P. & ZHAO, L.** 2003. Solubilization of Flurbiprofen in pH-Surfactant Solutions. *J. Pharm. Sci.*, 5 92, pp.951-956.
- LOFTSSON, T., HREINSDÓTTIR, D. & MÁSSON, M.** 2007. The complexation efficiency. *J. Incl. Phenom. Macrocycl. Chem.*, 57, pp.545-552.
- LOFTSSON, T., HREINSDÓTTIR, D. & MÁSSON, M.** 2005. Evaluation of cyclodextrin solubilization of drugs. *Int. J. Pharm.*, 302, pp.18-28.
- LUDWIG, D. S.** 2003. Dietary Glycemic Index and the Regulation of Body Weight. *Lipids*, 38, pp.117-121.
- MARSHALL, J. J. & MIWA, I.** 1981. Kinetic difference between hydrolyses of  $\gamma$ -cyclodextrin by human salivary and pancreatic  $\alpha$ -amylase. *BBA*, 661, pp.142-147.
- MARTINI, F. H.** 2004. *Fundamentals of Anatomy & Physiology*. 6<sup>th</sup> edition. San Fransisco: Pearson Education Inc.
- MILLER, G. L.** 1959. Use of Dinitrosalicylic Acid Reagent for Determination of Reducing Sugar. *Anal. Chem.*, 31 3, pp.426-428.
- MAAS, J., KAMM, W. & HAUCK, G.** 2007. An intergrated early formulation strategy - From hit evaluation to preclinical candidate profiling. *Eur. J. Pharm. Biopharm.*, 66, pp.1-10.
- ONG, J. K., SUNDERLAND, V. B. & MCDONALD, C.** 1997. Influence of hydroxypropyl  $\beta$ -cyclodextrin on the stability of benzylpenicillin in chloroacetate buffer. *J. Pharm. Pharmacol.*, 49, pp.617-621.
- ONYEJI, C. O., OMORUYI, S. I. & OLADIMEJI, F. A.** 2007. Dissolution properties and characterization of halofantrine-2-hydroxypropyl-beta-cyclodextrin binary systems. *Pharmazie*, 62, pp.858-863.
- PORTER, C. J. H., CHARMAN, S. A. & CHARMAN, W. N.** 1996. Lymphatic transport of halofantrine in the triple-cannulated anesthetized rat-model: Effect of lipid vehicle dispersion. *J. Pharm. Sci.*, 85, pp.351-356.
- PubChemCompound.** *Compound ID: 37393.* [online]. [Accessed Oktober 2010]. Available form World Wide Web: <http://pubchem.ncbi.nlm.nih.gov>
- REGIERT, M.** 2007. Oxidation-stable linoleic acid by inclusion in  $\alpha$ -cyclodextrin. *J. Incl. Phenom. Macrocycl. Chem.*, 57, pp.471-474.
- ROBYT, J. F. & FRENCH, D.** 1970. The Action Pattern of Porcine Pancreatic  $\alpha$ -Amylase in Relationship to the Substrate Binding Site of the Enzyme. *J. Biol. Chem.*, 245, pp.3917-3927.
- ROBYT, J. F. & FRENCH, D.** 1967. Multiple Attack Hypothesis of  $\alpha$ -Amylase Action: Action of Porcine Pancreatic, Human Salivary, and *Aspergillus oryzae*  $\alpha$ -Amylases. *Arch. Biochem. Biophys.*, 122, pp.8-16.

**SCHMID, R.** 2001. Recent Advances in the Description of the Structure of Water, the Hydrophobic Effect, and the Like-Dissolves-Like Rule. *Monatsh. Chem.*, 132, pp.1295-1326.

**SZEJTLI, J.** 1988. *Cyclodextrin Technology*. Dordrecht: Kluwer Academic Publishers.

**SZEJTLI, J.** 1998. Introduction and General Overview of Cyclodextrin Chemistry. *Chem. Rev*, 98, pp.1743-1753.

**TOKUMURA, T., UEDA, H., TSUSHIMA, Y., KASAI, M., KAYANO, M., AMADA, I., MACHIDA, Y. & NAGAI, T.** 1984a. Inclusion Complex of Cinnarizine with  $\beta$ -cyclodextrin in Aqueous Solution and in Solid State. *J. Inclusion Phenom.*, 2, pp.511-521.

**TOKUMURA, T., UEDA, H., TSUSHIMA, Y., KASAI, M., KAYANO, M., AMADA, I., MACHIDA, Y. & NAGAI, T.** 1984b. Inclusion Complexes of Cinnarizine with beta-cyclodextrin in Aqueous Solution and in the Solid State. *Chem. Pharm. Bull.*, 32, pp.4179-4184.

**UEDA, H., PERRIN, J. H. & NAGAI, T.** 1989. A microcalorimetric investigation of the binding of cinnarizine to cyclodextrins. *J. Pharmaceut. Biomed.*, 7, pp.639-642.

**UEKAMA, K.** 2004. Design and Evaluation of Cyclodextrin-Based Drug Formulation. *Chem. Pharm. Bull.*, 8 52, pp.900-915.

**UEKAMA, K., HIRAYAMA, F. & IRIE, T.** 1998. Cyclodextrin Drug Carrier Systems. *Chem. Rev.*, 98, pp.2045-2076.

**VAN DER MAAREL, M. J. E. C., VAN DER VEEN, B., UITDEHAAG, J. C. M., LEEMHUIS, H. & DUJKHUIZEN, L.** 2002. Properties and applications of starch-converting enzymes of the  $\alpha$ -amylase family. *J. Biotechnol.*, 94, pp.137-155.

**WESTERBERG, G. & WIKLUND, L.** 2005.  $\beta$ -Cyclodextrin Reduces Bioavailability of Orally Administered <sup>3</sup>[H]-Benzo[a]pyrene in the Rat. *J. Pharm. Sci.*, 1 94, pp.114-119.

**WISHART, D. S., KNOX, C., GUO, A. C., CHENG, D., SHRIVASTAVA, S., TZUR, D., GAUTAM, B. & HASSANALI, M.** 2008. *Drugcard for flurbiprofen*. [online]. [Accessed March 2010]. Available form World Wide Web: [www.drugbank.ca/drugs/DB00712](http://www.drugbank.ca/drugs/DB00712)

**WOLDUM, H. S., LARSEN, K. L. & MADSEN, F.** 2008. Cyclodextrin Controlled Release of Poorly Water-Soluble Drugs from Hydrogels. *Drug Deliv.*, 15, pp.69-80.

**ZANGENBERG, N. H., MÜLLERTZ, A., KRISTENSEN, H. G. & HOVGAARD, L.** 2001. A dynamic in vitro lipolysis model I. Controlling the rate of lipolysis by continuous addition of calcium. *Eur. J. Pharm. Sci.*, 14, pp.115-122.

## APPENDIX I

All compounds are of analytical grade unless otherwise stated.

### Buffer B:

Trizma® base, Sigma Aldrich, Mo, USA, Lot: 74H5706

Maleic acid, Sigma Aldrich, Mo, USA, Lot: 124K5424

NaCl, Merck, Germany, K40345104 932

CaCl<sub>2</sub>, AppliChem, Germany, 3H05234

NaOH, J.T. Baker, Holland, Lot: 0627503023

### HPLC run buffers:

Methanol, Sigma Aldrich, Mo, USA, HPLC grade

Acetonitrile, Sigma Aldrich, Mo, USA, HPLC grade

Sodium phosphate, Merck

### Compounds:

Ibuprofen, Sigma Aldrich, Mo, USA, Lot: 036k1620

Flurbiprofen, Sigma Aldrich, Mo, USA, Lot: 447994

Cinnarizine, Sigma Aldrich, Mo, USA, Lot: 048k1217

Danazol, Unikem, Denmark, Lot: 307870

Benzo[*a*]pyrene, Sigma Aldrich, Mo, USA, Lot: 097k1451

Halofantrine, kindly donated as the HCl salt by GSK (King of Prussia, NJ, USA), precipitated as the free base using the method of Porter *et al.* (1996)

### Cyclodextrins:

α-CD, ISP, Switzerland, Lot: 60P304

β-CD, Wacker, Germany, Lot: 71P013, pharmaceutical grade

γ-CD, Wacker, Germany, pharmaceutical grade

HP-β-CD, Cerestar, Lot: J8007

HP-γ-CD, ISP, UK, Lot 83p008

### DNS-solution:

3-5-dinitrosalicylic acid, Aldrich Chemical Company, WI, USA, Lot: 08728MG

NaOH, J.T. Baker, Holland, Lot: 0627503023

Potassium-sodium-tartrate, Merck, Germany, Lot: 945A465087

Sodium sulphite, Merck, Germany, Lot: K28344357

**Enzymes:**

Porcine pancreatic  $\alpha$ -amylase, type VI-B, Sigma Aldrich, MO, USA, Lot: 098k0730

Human pancreatic  $\alpha$ -amylase, Sigma Aldrich, MO, USA

Human salivary  $\alpha$ -amylase, type XIII-A type XIII-A, Sigma Aldrich, MO, USA



**APPENDIX II**

